ARTICLE IN PRESS

Cell Death & Disease

https://doi.org/10.1038/s41419-026-08536-0

Article in Press

GABAergic ventrolateral preoptic projection to dorsomedial hypothalamus recapitulates post-ischemic neuroprotection by hypothermia

Received: 12 August 2025

Revised: 20 February 2026

Accepted: 25 February 2026

Cite this article as: Dilsiz, P., Ozpinar, A., Balaban, B. *et al.* GABAergic ventrolateral preoptic projection to dorsomedial hypothalamus recapitulates post-ischemic neuroprotection by hypothermia. *Cell Death Dis* (2026). https://doi.org/10.1038/s41419-026-08536-0

Pelin Dilsiz, Aysenur Ozpinar, Buse Balaban, Halil İbrahim Koç, Serdar Altunay, Saltuk Buğra Baltacı, Fatma Zehra Hapil, Thorsten Roland Doeppner, Egor Dzyubenko, Mustafa Çağlar Beker, Dirk Matthias Hermann & Ertuğrul Kılıç

We are providing an unedited version of this manuscript to give early access to its findings. Before final publication, the manuscript will undergo further editing. Please note there may be errors present which affect the content, and all legal disclaimers apply.

If this paper is publishing under a Transparent Peer Review model then Peer Review reports will publish with the final article.

ARTICLE IN PRESS

© The Author(s) 2026. **Open Access** This article is licensed under a Creative Commons Attribution 4.0 International License, which permits use, sharing, adaptation, distribution and reproduction in any medium or format, as long as you give appropriate credit to the original author(s) and the source, provide a link to the Creative Commons licence, and indicate if changes were made. The images or other third party material in this article are included in the article's Creative Commons licence, unless indicated otherwise in a credit line to the material. If material is not included in the article's Creative Commons licence and your intended use is not permitted by statutory regulation or exceeds the permitted use, you will need to obtain permission directly from the copyright holder. To view a copy of this licence, visit http://creativecommons.org/licenses/by/4.0/.

ARTICLE IN PRESS

GABAergic ventrolateral preoptic projection to dorsomedial hypothalamus recapitulates post-ischemic neuroprotection by hypothermia

Pelin Dilsiz[1,2]*, Ayşenur Özpınar[2,3,4] †, Buse Balaban[2,5,6] †, Halil İbrahim Koç[2], Serdar Altunay[2,3], Saltuk Buğra Baltacı[2,3], Fatma Zehra Hapil[7], Thorsten Roland Doeppner[8,9], Egor Dzyubenko[10], Mustafa Çağlar Beker[11], Dirk Matthias Hermann[10]*, Ertuğrul Kılıç[11]*

*,† These authors contributed equally to this work.

* Corresponding author

Running head: vlPOA projection recapitulates hypothermic neuroprotection

ARTICLE IN PRESS

Author affiliations:

[1] Department of Molecular Biology and Genetics, Faculty of Science and Letters, Istanbul Technical University, Istanbul, Türkiye

[2] Research Institute for Health Sciences and Technologies (SABITA), Istanbul Medipol University, Istanbul, Türkiye

[3] Department of Physiology, School of Medicine, Istanbul Medipol University, Istanbul, Türkiye

[4] Graduate School of Health Sciences, Istanbul Medipol University, Istanbul, Türkiye

[5] Department of Medical Biology, School of Medicine, Istanbul Medeniyet University, Istanbul, Türkiye

[6] Department of Medical Biology, Institute of Health Sciences, University of Health Sciences, Istanbul, Türkiye

[7] Department of Medical Biology, Faculty of Medicine, Akdeniz University, Antalya, Türkiye

[8] University Medical Center Göttingen, Department of Neurology, Göttingen, Germany

[9] Klinikum Emden, Department of Neurology, Emden, Germany

[10] Department of Neurology, University Hospital Essen, University of Duisburg-Essen, Essen, Germany

ARTICLE IN PRESS

[11] Department of Physiology, School of Medicine, Istanbul Medeniyet University, Istanbul, Türkiye

*Correspondence:

Pelin Dilsiz, PhD

Department of Molecular Biology and Genetics

Istanbul Technical University

Istanbul, Türkiye

phone: +90-507-648-3699

email: perim@itu.edu.tr

ORCID: 0000-0001-9192-5014

Dirk M. Hermann, MD

Department of Neurology, University Hospital Essen

University of Duisburg-Essen

Essen, Germany

phone: +49-163-139-5330

email: dirk.hermann@uk-essen.de

ORCID: 0000-0003-0198-3152

Ertuğrul Kılıç, DVM PhD

Department of Physiology, School of Medicine

Istanbul Medeniyet University

Istanbul, Türkiye

phone: +90-530-349-1629

email: ertugrul.kilic@medeniyet.edu.tr

ORCID: 0000-0001-6494-8923

ARTICLE IN PRESS

ARTICLE IN PRESS

Abstract

Therapeutic hypothermia by exogenous cooling induces potent neuroprotection. Post-stroke, therapeutic hypothermia so far did not translate into clinically applicable therapies due to hypothermia-associated side-effects compromising patient outcome. The hypothalamus contains two major thermoregulatory centers in the ventrolateral preoptic area (vlPOA) and dorsomedial hypothalamus (DMH), which are connected via gamma-aminobutyric acid (GABA)-ergic fibers. Using chemogenetic and optogenetic approaches, we explored the role of this GABAergic projection in regulating body temperature responses, cerebral blood flow, and ischemic injury in *Vgat-cre* mice exposed to transient middle cerebral artery occlusion (MCAo). Using a chemogenetic approach we show that the inhibition of a set of GABAergic DMH^{VGAT} neurons, which under physiological conditions induces hyperthermia, is essential to drive hypothermia, which decreases cerebral blood flow post-MCAo and protects against ischemic reperfusion injury via mechanisms involving preservation of astrocytic homeostatic functions. This phenotype is recapitulated by the optogenetic activation of the GABAergic $vlPOA^{VGAT}$ neurons, which similarly induces hypothermia and protects against ischemic injury. The GABAergic $vlPOA^{VGAT}$ DMH pathway provides a potent target for neuroprotective therapies. We hypothesize that modulating central temperature responses via this pathway may not elicit the undesirable side effects associated with exogenous brain cooling.

Keywords: Dorsomedial hypothalamus, focal cerebral ischemia, gamma-aminobutyric acid, homeostatic astrocyte, therapeutic hypothermia, ventrolateral preoptic area

ARTICLE IN PRESS

ARTICLE IN PRESS

Introduction

Body temperature homeostasis is strictly regulated through thermoregulatory centers in the preoptic area and hypothalamus, which receive peripheral thermal signals and integrate them with endocrine, autonomic and behavioral information [1,2], providing a homeostatic feedback that maintains core body temperature (T_{core}) in a narrow range in homeothermic species [3–5]. Albeit the maintenance of T_{core} is crucial for various physiological functions, reducing T_{core} has broad clinical benefits under conditions of brain ischemia and trauma, since it promotes the survival of damaged brain tissue [6,7]. Therapeutic hypothermia induced by exogenous cooling potently decreases ischemic injury in experimental stroke models by regulating regional cerebral blood flow (CBF), oxidative stress and inflammation, in addition to maintaining blood-brain barrier (BBB) integrity [8–12].

Ischemic stroke is an eminent global health burden, which affects 1 in every 4 adults over the age of 25 [13], with increasing prevalence due to rising life expectancy [14,15]. Therapeutic hypothermia has been proposed to promote post-ischemic brain tissue survival in human patients [16–18] and improve neurological outcome of comatose subjects [19,20]. However, therapeutic hypothermia induced by exogenous or intraarterial cooling did not promote stroke outcome in randomized clinical trials, which was due to undesirable side effects, namely cardiac rhythm disturbances, hypokalemia, coagulopathy and infections, which outweighed the neuroprotective actions of hypothermia, preventing clinical patient recovery [21–25]. The quest for therapeutic strategies that enhance stroke outcome raises the need for treatments capable to induce neuroprotection in human stroke settings. Since several of the side effects above are likely associated with exogenous or intraarterial cooling, we here explored neural circuits in the hypothalamus that mediate hypothermia post-ischemia, aiming to define if these circuits might be suitable as a neuroprotective target.

Recently, a subset of dorsomedial hypothalamus (DMH) neurons expressing gamma-aminobutyric acid (GABA) was shown to receive robust input from GABAergic ventrolateral

ARTICLE IN PRESS

preoptic area (vlPOA) and regulate thermal information in mammals [26]. Upon deactivation, these DMH^{VGAT} neurons were found to induce hypothermia, which was also detected when the nerve terminals of GABAergic vlPOA neurons in the same brain region were activated [26]. DMH-projecting $vlPOA^{VGAT}$ neurons suppressed the thermogenic effects of DMH^{VGAT} neurons, which indicated the significance of the $vlPOA^{VGAT}$ → DMH pathway in thermoregulation [26]. The involvement of this pathway in post-ischemic neuroprotection was so far unknown. Given its central role in thermal information processing, we hypothesized that DMH-projecting GABAergic $vlPOA^{VGAT}$ neurons promote neuroprotection in the ischemic brain by inducing hypothermia. Herein, we demonstrate that chemogenetic inhibition of DMH^{VGAT} neurons and optogenetic activation of the $vlPOA^{VGAT}$ → DMH projection decreases T_{core} significantly, which in turn facilitates neurological recovery after focal cerebral ischemia evidenced by reduced infarct volume and neuronal reperfusion injury. The $vlPOA^{VGAT}$ → DMH pathway provides a promising target for neuroprotection therapies.

ARTICLE IN PRESS

Materials and methods

Legal aspects

This study has been conducted under the ethics standards of the EU Guidelines on the Care and Use of Laboratory Animals (Directive 2010/63/EU) in agreement with Turkish National guidelines for animal experimentation. The study has been approved by local animal experimentation authorities (Animal Research Ethics Committee, Istanbul Medipol University; reference number: 01/12/2021-75).

Animal holding and study blinding

ARTICLE IN PRESS

Experimental procedures are reported in accordance with ARRIVE guidelines (Animal Research: Reporting of In Vivo Experiments). Male Cre-recombinase expressing *Vgat-cre* mice *(Slc32a1*$^{tm2(cre)Lowl}$/J, stock 016962; Jackson Labs, Bar Harbor, ME, USA) back-crossed with C57Bl/6 mice (Stock 000664; Jackson Labs) were housed in a 12-hour light (07:00-19:00) and dark (19:00-07:00) cycle at 22-24°C ambient temperature, having *ad libitum* access to standard food and water. At the age of 8-12 weeks (20-25 g), mice were randomly assigned to experimental groups by sequential allocation, ensuring balanced animal numbers on each surgery day. Experimenters were blinded to group allocation at all stages of the study (animal experiments, histochemical stainings and data analysis). Animal welfare was monitored daily throughout the study. Mice exhibiting a body weight reduction following adeno-associated virus (AAV) vector injection to below 20 g at the time of MCAo were excluded from the study.

Statistical planning

Statistical planning was done by a sample size calculator (https://clincalc.com/stats/samplesize.aspx). Assuming an alpha error of 5% and a beta error (1–statistical power) of 20%, these calculations determined that 8 animals were needed per group for behavioral and histochemical analyses, provided that the mean value was modified by 35% and that the standard deviation of the data sample was 25% of the mean value (effect size: 1.4). To account for animal dropouts, 10 animals per group were stereotactically injected throughout the study.

Adeno-associated virus (AAV) production

Recombinant AAV production was performed as described previously [27]. Cre-dependent recombinant AAV vectors purchased from http://www.addgene.org/ were used as follows: *rAAV2/1-CAG-DIO-GFP* (10^{14} vg/mL), *rAAV2/1-EF1a-DIO-hM4D(Gi)-mCherry* ($4x10^{12}$ vg/mL) and *rAAV2/1-EF1a-DIO-hChR2(H134R)-EYFP-WPRE-HGHpA* ($1.8x10^{14}$ vg/mL) (*CAG:*

ARTICLE IN PRESS

cytomegalovirus (CMV) enhancer/chicken beta-actin promoter, EF1a: *human elongation factor-1 alpha* promoter, *DIO*: *double-floxed inverted open-reading frame*).

Stereotactic viral injections and optical fiber implantation

Viral injections were performed as described previously [28–30]. Briefly, P30-P40 mice were anesthetized with 1% isoflurane (30% O_2, 70% N_2O) and placed in a stereotactic instrument (David Kopf Instruments, Tujunga, CA, USA). After a skin incision, the animals' skull was exposed and trephinated using a small drill for stereotactic injection. A total of 600 nl virus was injected intracranially to each side using a pulled glass pipette (Wiretrol; Drummond Scientific, Broomall, PA, USA) with a 50 µm tip diameter. Injections were performed into the DMH (bregma: -1.50 mm, midline: ± 0.35 mm, dorsal surface: -4.90 mm) and vlPOA (bregma: -0.10 mm, midline: ± 0.70 mm, dorsal surface: -5.60 mm) at a rate of 30 nL/min using a micromanipulator (Narishige, East Meadow, NY, USA), allowing 10 min for each injection. For *in vivo* photostimulation, a ferrule capped optical fiber (200 µm core diameter, NA = 0.50, ThorLabs) was implanted above the DMH (bregma: -1.50 mm, midline: ± 0.35 mm, dorsal surface: -4.40 mm) after viral injections. The ferrules were fixed with dental cement, and the mice were allowed to recover for at least 3 weeks.

Clozapine injection and photostimulation

For chemogenetic stimulation, 0.3 mg/kg clozapine (Tocris Bioscience, Bristol, UK) or normal saline was intraperitoneally (i.p.) administered to $DMH^{VGAT:hM4D}$ designer receptors exclusively activated by designer drugs (DREADD) mice or $DMH^{VGAT:GFP}$ non-DREADD control mice[30,31] obtained by rAAV mediated transduction. *In vivo* photostimulation of DMH-projecting $vlPOA^{VGAT}$ neurons was performed using a 473 nm diode laser (Doric Lenses Inc., Quebec City, Canada) through a ferule-capped optical fiber implanted in $vlPOA^{VGAT:ChR2}$ or $vlPOA^{VGAT:GFP}$ mice[30,31] obtained by rAAV mediated transduction using the following stimulation protocol: 10 Hz stimuli with 10 ms pulse length were applied for 1 second; this stimulus was repeated every 4

ARTICLE IN PRESS

seconds [30]. Optical stimulation was started 30 min before MCAO and continued until the end of MCAO, i.e., onset of reperfusion.

Behavioral studies

Body temperature measurement

Body core temperature (T_{core}) was recorded using a thermocouple rectal probe and thermometer (Physitemp Instruments, Clifton, NJ, USA). T_{core} of $DMH^{VGAT:hM4D}$ or $DMH^{VGAT:GFP}$ mice was measured for 30 min at baseline. Then, 0.3 mg/kg clozapine was administered, and T_{core} was recorded for 3 hours. In the meantime, T_{core} was measured using an infrared fusion thermal camera (Ti90; Fluke, Everett, WA, USA). Snapshot images were taken at the specified time points, and an average of 3 recordings was obtained. Similarly, T_{core} was recorded using the thermocouple rectal probe in $vlPOA^{VGAT:ChR2}$ or $vlPOA^{VGAT:GFP}$ mice during a 30 min baseline recording and subsequent 2 hours photostimulation. T_{core} was also assessed using the infrared fusion thermal camera. Snapshot images were obtained.

Neurological score

In mice exposed to 90 min MCAo, neurological deficits were evaluated using the 5-point Bederson score at 24 hours after reperfusion. In this score, 0 reflects normal function, 1 reflects flexion of the torso and contralateral forelimb upon lifting the animal by the tail, 2 reflects circling to the contralateral side but normal posture at rest, 3 reflects reclination to the contralateral side at rest, and 4 reflects absence of spontaneous motor activity.

Open field test

Following a post-operative recovery period, mice exposed to 30 min MCAo were transferred to the testing room and single-housed in Coulbourn Habitest cages (Coulbourn Instruments, Allentown, PA, USA) in cotton bedding without being handled for 3 days. The investigator then

ARTICLE IN PRESS

handled the mice for 3 days to reduce stress. The circular test chamber, having a 100 cm diameter and surrounded by a 35 cm tall sidewall, was divided into three sections, including an outer wall zone (17.7% of diameter, close to the wall), an intermediate transition zone (32.3% of diameter), and an inner zone (50% of diameter, the center of the chamber) [32,33]. On the test days, animals were placed in an open field test chamber 30 min after clozapine or saline administration and observed for 10 min. The assay was traced with a CCF camera and blindly analyzed by two researchers using ANY-maze software (Version 4.99; Stoelting Co., Dublin, Ireland).

Focal cerebral ischemia induction

Focal cerebral ischemia was induced by intraluminal middle cerebral artery occlusion (MCAo) as described previously [34]. To initiate chemogenetic inhibition of DMH^{VGAT} neurons, 0.3 mg/kg clozapine was intraperitoneally administered to $DMH^{VGAT:hM4D}$ or $DMH^{VGAT:GFP}$ mice 30 min before MCAo, whereas optogenetic activation of $vlPOA^{VGAT}$ → DMH fibers was provided via photostimulation starting with MCAo until animal sacrifice. Mice were deeply anesthetized with 1% isoflurane (30% O_2, remainder N_2O), and their T_{core} was monitored using a feedback-controlled heating system (Harvard Apparatus, Holliston, MA, USA). CBF was measured and monitored by Laser Doppler flow (LDF) measurement using a flexible 0.5 mm fiber optic probe (PIMSoft; Perimed, Järfälla, Sweden). The optic probe was attached to the skull above the core of the middle cerebral artery territory (2 mm posterior/ 6 mm lateral from the bregma). Following a neck incision, the left common and external carotid arteries were isolated and ligated and a microvascular clip (FE691; Aesculap, Tuttlingen, Germany) was temporally placed on the internal carotid artery. A 7.0 silicon-coated nylon monofilament (701934PK5Re; Doccol, Sharon, MA, USA) was subsequently inserted into the common carotid artery through a narrow incision and advanced 9 mm distal to the carotid bifurcation for MCAo.

90 or 30 min after the onset of ischemia, reperfusion was induced by monofilament removal. At 24 hours after reperfusion, mice exposed to 90 min MCAo were decapitated under deep

ARTICLE IN PRESS

anesthesia. The brains were collected and immediately frozen on dry ice. 18 µm thick coronal sections were obtained using a cryostat (CM1950; Leica, Wetzlar, Germany) and subsequently used to analyze infarct size, brain edema, and IgG extravasation. Mice exposed to 30 min MCAo were transcardially perfused in deep anesthesia at 72 hours after reperfusion using 0.1 M 0.1 M pH 7.4 phosphate-buffered saline (PBS) followed by 4% paraformaldehyde (PFA) in 0.1 M pH 7.4 PBS. Brains were harvested, post-fixed in the same fixative for 4 hours, and transferred to a 30% sucrose solution overnight. 75 µm brain sections were collected with a vibratome (VT1000S; Leica) for immunohistochemistry.

Laser speckle imaging

CBF was also evaluated by laser speckle imaging in $DMH^{VGAT:hM4D}$ or $DMH^{VGAT:GFP}$ mice intraperitoneally treated with clozapine (0.3 mg/kg). Anaesthetized mice were placed in a stereotactic instrument. A CCD camera was located approximately 10 cm above the brain to detect CBF variations using a Pericam PSI System (PIMSoft; Perimed) using a 785 nm wavelength laser, which penetrates approximately 500 µm deep into the brain surface. Speckle images were collected every 2 seconds with 20 µm spatial image resolution. The regional CBF was recorded for 90 min, the mean CBF was calculated by blood perfusion imaging software (PIMsoft; Perimed), and changes in relative CBF were calculated.

Evaluation of infarct volume, brain edema, and serum IgG extravasation

Infarct volume and brain edema were evaluated at millimeter intervals across the forebrain in animals exposed to 90 min MCAo. Brain sections were stained with cresyl violet [35]. ImageJ software (National Institute of Health, Bethesda, MD, USA) was used for infarct measurements, outlining healthy tissue in both hemispheres, which were subtracted from each other for infarct area measurement. Infarct volume was obtained by integrating infarct areas at various rostro-caudal brain levels. Brain edema was calculated by subtracting areas of the contralateral

ARTICLE IN PRESS

hemisphere from areas of the ischemic hemisphere at the level of the bregma (which is the core of the middle cerebral artery territory) and dividing the resulting values by the corresponding areas of the contralateral hemisphere. Infarct volume was defined as primary outcome of this study in mice exposed to 90 min MCAo, whereas brain edema and all subsequently listed readouts were regarded as secondary outcomes.

In 90 min MCAo mice, brain sections collected from the bregma level were rinsed with 0.1 M PBS to remove intravascular IgG, fixed in 4% PFA and blocked with methanol/ 0.3% H_2O_2. Sections were then immersed in 5% bovine serum albumin (BSA) and normal swine serum (1:1000) in 0.1 M PBS and incubated for 1 hour in biotinylated goat anti-mouse IgG (sc-2013; Santa Cruz Biotechnology, Santa Cruz, CA, USA). After staining with avidin peroxidase kit (Vectastain Elite; Vector Labs, Newark, CA, USA) and diaminobenzidine (Sigma-Aldrich, St. Louis, MO, USA), IgG extravasation in the ischemic striatum was analyzed densitometrically using Image J software. The optical densities of corresponding contralateral non-ischemic tissue were subtracted from those in the ischemic tissue for background staining correction.

ARTICLE IN PRESS

Immunohistochemistry and microscopy

Brain sections obtained from the level of the bregma of 30 min MCAo mice were blocked in 0.1 M PBS containing 0.1 mM Triton-X100 (PBS-T) and 5% normal goat serum for 1 h at room temperature. Sections were subsequently immersed in blocking solution containing monoclonal mouse anti-pyruvate kinase M2 (PKM2) (1:300; sc-365684; Santa Cruz Biotechnology), monoclonal rabbit anti-Bcl-xL (1:500; 2764; Cell Signaling, Danvers, MA, USA), monoclonal rat anti-GFAP (1:500; 13-0300; Thermo-Fisher Scientific, Waltham, MA, USA), polyclonal rabbit anti-c-Fos (1:000; 2250; Santa Cruz Biotechnology), Alexa Fluor 488-conjugated monoclonal mouse anti-NeuN (1:100; MAB377; Merck-Millipore, Burlington, MA, USA), or Alexa Fluor 555-conjugated monoclonal mouse anti-GFAP (1:100; 3656; Cell Signaling) antibodies. After an overnight incubation at 4°C, brain sections were rinsed with PBST. Sections exposed to non-

ARTICLE IN PRESS

conjugated primary antibodies were then exposed to Alexa Fluor 488-conjugated secondary antibody (1:500; A11001; goat anti-mouse IgG (H+L); Invitrogen, Waltham, MA, USA), Alexa Fluor 488-conjugated secondary antibody (1:500; A11008; goat anti-rabbit IgG (H+L), Invitrogen) Alexa Fluor 568-conjugated secondary antibody (1:500; A11011; goat anti-rabbit IgG (H+L), Invitrogen) or Alexa Fluor 594-conjugated secondary antibody (1:500; A11007; goat anti-rat IgG (H+L), Invitrogen) for 1 h at room temperature. Brain sections were again rinsed with PBST. Sections were counterstained with 4′, 6-diamidino-2-phenylindole (DAPI) and mounted with Fluoromount (F4680; Sigma Aldrich). Additional brain sections were labeled with terminal transferase dUTP nick end labeling (TUNEL) kit (In Situ Cell Death Detection Kit; Roche, Basel, Switzerland) to detect neuronal injury through DNA fragmentation. Imaging was performed by confocal microscopy (Carl Zeiss, Jena, Germany). Nine different regions of interest (ROIs) from the striatum, each measuring 62,500 μm^2, were evaluated to detect neuronal survival and injury. $NeuN^+$ cells or DNA fragmented cells were analyzed in the ischemic and contralateral striatum. Neuronal survival was evaluated by dividing the density of $NeuN^+$ surviving neurons in both hemispheres. Astrocytic responses were evaluated by measuring the total area of GFAP immunoreactivity in the ischemic hemisphere. To measure PKM2 and Bcl-xL expression levels in astrocytes and non-astrocytic cells, binary masks representing $GFAP^+$ astrocytes were generated by manual thresholding in ImageJ Software. Average signal intensities were measured within (for astrocytes) and outside of (non-astrocytic cells) the masks. Neuronal survival was defined as primary outcome of this study in mice exposed to 30 min MCAo, whereas all other readouts were considered as secondary outcomes.

Statistical analysis

All results were shown as mean ± SEM values. Differences between two groups were tested by two-tailed unpaired Student's t tests after confirming normal distribution using Shapiro-Wilk tests. Non-normally distributed data were evaluated using Mann-Whitney U tests (Statistical Table 1). P

ARTICLE IN PRESS

values were calculated using Prism 9.5 (GraphPad Software Inc.). Outlier tests were removed only when data deviated more than two standard deviations from mean values. p values < 0.05 were considered as statistically significant.

Results

Chemogenetic silencing of GABAergic DMH^{VGAT} neurons induces hypothermia

GABAergic neurons residing in the DMH were previously shown to drive hypothermia upon inhibition and promote thermogenesis when activated [26]. To gain insight into their role of central body temperature control, we stereotactically administered a Cre-dependent *rAAV2/1-EF1a-DIO-hM4D(Gi)-mCherry* in the DMH of *Vgat-cre* mice (Fig. 1). Chemogenic inhibition of GABAergic DMH^{VGAT} neurons by clozapine (Fig. 2A and 2B) significantly decreased core body temperature by 1.95 ± 0.11 °C in DIO-hM4D DREADD mice compared to mice receiving a non-DREADD (DIO-GFP) control vector, confirming the involvement of DMH^{VGAT} neurons in T_{core} regulation (Fig. 2C, D). Furthermore, we showed that locomotor activity decreased upon the chemogenetic silencing of DMH^{VGAT} neurons (Fig. 2E-H), which represents a homeostatic response towards temperature changes. Upon careful inspection, we did not observe any behavioral abnormalities upon chemogenetic DMH^{VGAT} silencing in this study. Our data argue in favor of a specific thermoregulatory response.

DMH^{VGAT} silencing reduces infarct volume, neurological deficits and brain edema

Considering that chemogenetic silencing of GABAergic DMH^{VGAT} neurons reduced body temperature, we next investigated whether DMH^{VGAT} silencing induces neuroprotection after ischemic stroke induced by 90 min MCAo (Fig. 3A, Supplementary Fig. S1A), which was earlier shown to induce focal infarcts in the striatum and the overlying cortex, in addition to moderate brain edema of the ischemic hemisphere compared to contralateral hemisphere [35–37]. Chemogenetic DMH^{VGAT} silencing significantly reduced infarct volume in DIO-hM4D mice at 24

ARTICLE IN PRESS

hours post-MCAo (Fig. 3B). Similarly, chemogenetic DMH^{VGAT} silencing reduced brain swelling (Fig. 3C) and BBB leakage measured by IgG extravasation (Fig. 3D), although the latter effects lacked to show statistical significance. Neurological deficits examined by the Bederson score were significantly reduced by DMH^{VGAT} silencing (Fig. 3E). Taken together, our findings demonstrate that DMH^{VGAT} silencing robustly improved neurological outcome after stroke.

DMH^{VGAT} silencing increases post-ischemic neuronal survival and preserves the astrocytic homeostatic state

We have previously shown that disseminate neuronal injury can be detected in the ischemic striatum when mice are exposed to 30 min MCAo [35,37]. Earlier studies revealed that this type of cell injury evolves over up to 72 hours post-MCAo and that it mostly affects small- to medium-sized interneurons [38,39]. Therefore, we next investigated whether hypothermia induced by chemogenetic DMH^{VGAT} silencing increases neuronal survival in the striatum of 30 min MCAo mice (Fig. 4A, Supplementary Fig. S1B). Indeed, DMH^{VGAT} silencing promoted neuronal survival in this mild ischemic brain injury model (Fig. 4B, C, Supplementary Fig. S2A). Thus, the percentage of surviving NeuN^{+} neurons was increased in DMH^{VGAT} silenced DIO-hM4D compared to non-silenced DIO-GFP mice (Fig. 4B, C).

Astrocytes support brain homeostasis under physiological conditions, but exhibit inflammatory changes post-ischemia associated with GFAP immunoreactivity [40,41], which provides the basis for subsequent glial scar development [42]. We thus investigated the impact of chemogenetic DMH^{VGAT} silencing on astrocytic GFAP responses following 30 min MCAo, showing that DMH^{VGAT} silencing decreased the area of brain tissue covered by GFAP^{+} reactive astrocytes (Fig. 4B, D).

Under homeostatic conditions, astrocytes take up glutamate from the extracellular space and detoxify the brain tissue [43]. Upon ischemia, astrocytes may adopt a neurotoxic state characterized by compromised mitochondrial function that is predominated by lactate-directed

ARTICLE IN PRESS

glycolysis [44]. PKM2, which regulates mitochondrial function [45], plays a central role in the metabolic switch of homeostatic astrocytes to neurotoxic astrocytes [44]. Given that PKM2 is upregulated upon ischemia [46], we investigated the expression of PKM2 in GFAP$^+$ astrocytes. Indeed, astrocytes exhibited robust cytosolic PKM2 expression post-ischemia, and PKM2 levels markedly decreased in response to hypothermia induced by DMH^{VGAT} silencing (Fig. 4E-G). Notably, this reduction was not restricted to GFAP$^+$ astrocytes but was also evident in GFAP$^-$ cell populations, which presumably involved non-astrocytic cell populations (Fig. 4E-G). In addition to its anti-apoptotic role, Bcl-xL maintains mitochondrial function in astrocytes [47]. We next investigated whether hypothermia induced by DMH^{VGAT} silencing increases Bcl-xL levels in the ischemic brain. Bcl-xL and GFAP immunostaining confirmed that Bcl-xL levels increased upon DMH^{VGAT} silencing, but only modestly in astrocytes (Supplementary Fig. S2A, B). Taken together, our findings indicate that hypothermia induced by chemogenetic DMH^{VGAT} silencing promotes neuronal survival by preservation of the homeostatic astrocyte state.

DMH^{VGAT} silencing reduces post-ischemic reperfusion and decreases reperfusion injury

Vasoconstriction is one of the most critical responses, via which mammals cope with hypothermia [48]. Considering that vasoconstriction-associated CBF reduction may protect the brain against neuronal injury by reducing oxidative stress [49,50], we next examined if chemogenetic DMH^{VGAT} silencing influenced post-ischemic reperfusion. To test this, laser speckle imaging was performed in *Vgat-cre* mice. Regional CBF was monitored during 30 min MCAo followed by 60 min reperfusion (Fig. 5A). Our findings revealed that the chemogenetic deactivation of DMH^{VGAT} neurons potently decreased regional CBF during reperfusion in the ischemic core and penumbra regions in DIO-hM4D compared to DIO-GFP mice (Fig. 5B-D). Of note, regional CBF very slowly recovered over the one-hour-interval post-ischemia in hypothermic DMH^{VGAT} silenced mice. We conclude that chemogenetically induced hypothermia protects against ischemia by preventing cerebral reperfusion injury.

ARTICLE IN PRESS

To elucidate how chemogenetic DMH^{VGAT} silencing influences reperfusion injury in the previously ischemic striatum, we subsequently evaluated irreversible cell injury by DNA fragmentation analysis. Our findings revealed that chemogenetic deactivation of DMH^{VGAT} neurons decreased the number of DNA fragmented cells indicative of reduced reperfusion injury (Fig. 5E, F).

Optogenetic activation of the GABAergic vlPOA^{VGAT} → DMH pathway induces hypothermia

Previous studies demonstrated that DMH receives dense GABAergic inputs from the vlPOA, which contribute to hypothalamic core body temperature regulation [26]. To gain insight into the role of DMH-projecting vlPOA^{VGAT} neurons in hypothermia induction, we transduced GABAergic neurons located in the vlPOA of *Vgat-cre* mice by administering a Cre-dependent *rAAV2/1-EF1a-DIO-hChR2(H134R)-EYFP-WPRE-HGHpA* vector. Transduction of vlPOA^{VGAT} neurons by DIO-hChR2 yielded robust axonal labeling in the DMH (Fig. 6A). Optogenetic activation of vlPOA^{VGAT} → DMH neurons induced the co-expression of eYFP and c-Fos in vlPOA^{VGAT} synapses of DIO-hChR2 mice (Fig. 6B). We subsequently investigated the role of the vlPOA^{VGAT} → DMH projection in core body temperature regulation by stimulating vlPOA^{VGAT} terminals in the DMH using 473 nm laser light pulses. Here, we found that optical stimulation significantly reduced T_{core} by 2.02 ± 0.34 °C (Fig. 6C, D), which suggested that activation of vlPOA^{VGAT} terminals recapitulated the effect of DMH^{VGAT} silencing. Upon careful inspection, we did not observe any behavioral abnormalities upon optogenetic vlPOA^{VGAT} activation, emphasizing the specificity of the temperature response. Collectively, the functional findings obtained indicated that vlPOA^{VGAT} neurons induce hypothermia by inhibiting DMH^{VGAT} neurons.

vlPOA^{VGAT} → DMH pathway activation induces post-ischemic neuroprotection and preserves astrocytic homeostasis

ARTICLE IN PRESS

Given the involvement of DMH-projecting vlPOA^{VGAT} neurons in inducing hypothermia, we further asked whether activation of this pathway is able to phenocopy the effects of chemogenetic DMH^{VGAT} silencing on ischemic brain tissue survival. For this, we again induced 90 min occlusion to introduce focal infarcts (Supplementary Fig. S1C). Optogenetic activation of the vlPOA^{VGAT} → DMH projection reduced ischemic injury at 24 hours post-MCAo. Indeed, infarct volume and brain edema were significantly reduced by vlPOA^{VGAT} → DMH activation (Fig. 7A, B), whereas BBB leakage evaluated by IgG extravasation was modestly, but non-significantly decreased (Fig. 7C). Taken together, activating the nerve terminals of DMH-projecting vlPOA^{VGAT} neurons mimics the effects of DMH^{VGAT} silencing on ischemic brain injury.

We next investigated whether optogenetic activation of the vlPOA^{VGAT} → DMH pathway similarly provided neuroprotection following mild ischemic injury induced by 30 min MCAo (Supplementary Fig. S1D). Indeed, we observed decreased disseminate cell injury assessed by TUNEL (Fig. 7D, E). NeuN immunostaining revealed that optogenetic activation of vlPOA^{VGAT} → DMH projecting nerve terminals increased neuronal survival in the striatum 72 hours after 30 min MCAo (Fig. 8A, B). Optogenetically induced hypothermia reduced post-ischemic astrocyte reactivity and neurotoxicity, as indicated by the downregulated GFAP and PKM2 expression (Fig. 8A, C-E). Additionally, we observed decreased expression of PKM2 and Bcl-xL in GFAP^{-} cells (Fig. 8F, Supplementary Fig. S2C, D), suggesting adaptive mitochondrial regulation in non-astrocytic cells. These findings indicate that hypothermia induced by optogenetic vlPOA^{VGAT} → DMH pathway activation preserves the homeostatic role of astrocytes and promotes neuronal survival after stroke.

Discussion

Multiple lines of evidence suggest that mild hypothermia potently promotes neuronal survival and prevents cell death in experimental brain injury, including ischemic stroke models [51–55]. So far, therapeutic hypothermia induced through systemic and intra-arterial cooling failed to enhance

ARTICLE IN PRESS

neurological outcome in ischemic stroke patients in randomized clinical trials, which was due to multiple side-effects, namely cardiac rhythm disturbances, hypokalemia, coagulopathy and infections, which compromised stroke recovery [21–25,56–58]. In view of the persisting deficits of stroke patients in the post-acute stroke phase, there is a need for treatments that enhance stroke recovery. Given the strong neuroprotective effect induced by the activation of the GABAergic vlPOA^{VGAT} pathway to the DMH, this pathway might provide a promising target for treatments that enhance stroke outcome. Indeed, optogenetic activation of vlPOA^{VGAT} neurons potently induced hypothermia in *Vgat-cre* mice, as did chemogenetic silencing of DMH^{VGAT} neurons, both of which induced neuroprotection by inhibiting cerebral reperfusion injury.

The maintenance of body temperature is critical for cell survival and homeostasis. Body temperature regulation is strictly orchestrated by thermoregulatory networks in the anterior and dorsomedial hypothalamus [26,59], which integrate peripheral thermal, endocrine, autonomic and behavioral information [3,4]. Involvement of the DMH in thermal information processing has been suggested in studies showing that DMH^{VGAT} neurons induced thermogenesis when activated chemogenetically [26]. Conversely, optogenetic silencing of DMH^{VGAT} neurons was found to induce hypothermia [26]. Consistent with earlier studies, our study showed that chemogenetic DMH^{VGAT} silencing potently decreases T_{core}, which goes in line with reduced physical activity. In contrast to our study and the above earlier studies, a recent study did not observe T_{core} changes when GABAergic DMH neurons were optogenetically activated over a shorter time interval [60]. In view of this apparent dependency on the duration and timing of the therapeutic intervention, we initiated chemogenetic DMH^{VGAT} silencing before MCAo and retained it until the end of the occlusion to ensure a significant loss of body temperature.

Warm-sensitive neurons in the preoptic area are a key sensor and regulator of thermal homeostasis [61,62] that project to distinct effector regions in the brain to regulate brown adipose tissue activity and skin vasodilation [26,59]. The preoptic area integrates inputs from ascending thermoregulatory pathways in the brainstem and spinal cord that convey information from the

ARTICLE IN PRESS

body periphery [63,64]. Interestingly, tracing studies showed that the vlPOA provides a significant projection to the DMH [65,66]. GABAergic neurons in the vlPOA were shown to evoke tonic inhibition of brown adipose tissue activity via the DMH [67,68], whereas pharmacological inhibition of $GABA_A$ receptors in the DMH stimulated brown adipose tissue activity by sympathetic activation [69,70]. Previously, GABAergic neurons located at the vlPOA were found to suppress cold-activated DMH ^{VGAT} neurons to lower core body temperature [26]. Consistent with this study, we demonstrated that the DMH receives robust input from vlPOA^{VGAT} neurons. We found that optogenetic activation of vlPOA^{VGAT} originating nerve terminals in the DMH similarly as chemogenetic DMH^{VGAT} silencing potently induced hypothermia.

Our study shows that chemogenetic DMH^{VGAT} neuron silencing and optogenetic activation of GABAergic vlPOA^{VGAT} fibers terminating in the DMH induced hypothermia in *Vgat-cre* mice to reduce infarct volume, brain edema, neurological deficits, reactive astroglial responses and cerebral reperfusion injury. Upon careful inspection, we did not observe any behavioral abnormalities associated with chemogenetic and optogenetic interventions in this study. Therapeutic hypothermia induced by animal cooling potently has previously been shown to decrease ischemic injury in experimental stroke models by regulating CBF, decreasing oxidative stress and inflammation, and preserving BBB integrity [8–12]. Our data indicate that hypothermia induced by the optogenetic activation of the GABAergic vlPOA^{VGAT} → DMH pathway recapitulates these effects, as does chemogenetic DMH^{VGAT} silencing.

Astrocytes are key for homeostatic responses to brain injury [43]. After stroke, astrocytes undergo inflammatory changes associated with GFAP immunoreactivity [40,41], which provides the basis for subsequent glial scar development [42]. Reprogramming in ischemic astrocytes can be both beneficial (neuroprotective) and detrimental (neurotoxic) [40,41,71].Previously, activation of the PKM2-STAT3-hypoxia-inducible factor (HIF) pathway has been described as a key trigger of astrocytic neurotoxicity after stroke [44]. Metabolic reprogramming in ischemic astrocytes induces PKM2-mediated phosphorylation and activation of transcriptional factor STAT3, which in turn

ARTICLE IN PRESS

induces HIF expression. Activation of hypoxia-responsive elements for HIF promotes PKM2 expression, creating the “vicious cycle” of neurotoxic astrocytic remodeling. In this study, we demonstrate that hypothermia induced by both chemogenetic DMH^{VGAT} silencing and optogenetic $vlPOA^{VGAT}$ → DMH activation downregulates PKM2 expression in neurotoxic astrocytes, contributing to post-ischemic brain tissue survival.

Cold exposure has long been known to induce vasoconstriction [48,72]. Two aspects explain the lowering of blood flow in hypothermia, which is the need of counteracting heat loss through the body surface and the reduction of cell metabolism requiring less oxygen and energy-rich substrates to be provided via the blood. In the present study, we found markedly reduced post-ischemic regional CBF in the brains of mice exhibiting chemogenetic DMH^{VGAT} deactivation. The reduction of energy consumption post-ischemia protects the brain, since it reduces cerebral cellular reperfusion injury. Of note, we indeed observed reduced disseminate cell death in the brains of mice receiving chemogenetic DMH^{VGAT} silencing and optogenetic $vlPOA^{VGAT}$ → DMH activation, which supports this mechanism. That tissue reperfusion in animals undergoing transient focal cerebral ischemia may augment brain injury above levels observed in permanent focal cerebral ischemia is well established [73,74]. Our data suggest that therapeutic hypothermia induced by DMH^{VGAT} deactivation and $vlPOA^{VGAT}$ → DMH activation counteracts the post-ischemic reperfusion injury, enabling successful recovery of the brain tissue.

A limitation of our study is the initiation of hypothermia on occasion of the stroke onset. However, we did not directly test the effect of post-ischemic hypothermia induced by chemogenetic DMH^{VGAT} silencing and optogenetic $vlPOA^{VGAT}$ → DMH activation. Future experiments will have to define therapeutic windows of chemogenetically and optogenetically induced neuroprotection. The model used is a clinically relevant model of post-ischemic reperfusion damage, which following recent advances in reperfusion therapies (thrombolysis combined with mechanical thrombectomy) has gained clinical importance. We did not test the effect of hypothermia induced by DMH^{VGAT} neuron silencing and $vlPOA^{VGAT}$ → DMH pathway

ARTICLE IN PRESS

activation on female animals and aged animals with vascular risk factors or comorbidities. Future studies will have to elucidate long-term outcomes in mice with chemogenetically or optogenetically induced hypothermia.

In summary, we herein identified a GABAergic vlPOA^{VGAT} → DMH pathway, which mediates potent neuroprotection in mice exposed to transient MCAo. In view of the well-defined temperature response, this projection may provide a potent target for neuroprotection not only in ischemic stroke, but also in other brain injury conditions, including cardiac arrest, traumatic brain injury, subarachnoid hemorrhage or intracerebral hemorrhage. Transcranial magnetic stimulation techniques have made huge progress in recent years, and it is meanwhile possible to stimulate deep brain structures in a localized way [75]. We predict that via stimulation of the vlPOA^{VGAT} → DMH pathway, it might be possible to enhance clinical outcome of brain-injured patients. Since this procedure does not involve exogenous peripheral or intra-arterial cooling, this treatment has the potential of bypassing the side effects previously noted in randomized controlled hypothermia trials, in which cardiac rhythm disturbances, hypokalemia, coagulopathy and infections compromised clinical outcome of ischemic stroke patients [21–25]. Experimental studies are warranted on this topic.

ARTICLE IN PRESS

ARTICLE IN PRESS

Conflict of Interest

The authors declare no competing interests.

Availability of Data and Materials

The datasets generated and analyzed during the current study are available from the corresponding author upon reasonable request.

Acknowledgements

We thank Dr. Deniz Atasoy from The University of Iowa for critical reading of the manuscript and Dr. Zuhal Er from Istanbul Technical University for providing thermal imaging instrumentation.

Author contributions

P.D., A.O. and B.B. performed optogenetic and chemogenetic manipulations. B.B. produced rAAV and A.O. performed intracranial injections. S.A. performed middle cerebral artery occlusion surgeries. A.O. and H.I.K performed behavioral tests. A.O., B.B. and S.B.B. performed imaging. F.Z.H. and E.D. performed astrocyte colocalization analysis. P.D., F.Z.H. and M.C.B. analyzed the data. P.D. prepared figures. P.D., M.C.B., T.R.D., D.M.H., and E.K. conceived experiments and prepared the paper. All authors critically revised it.

ARTICLE IN PRESS

ARTICLE IN PRESS

References

1 Nakamura K, Morrison SF. A thermosensory pathway that controls body temperature. *Nat Neurosci* 2008; **11**: 62–71.

2 Nakamura K, Morrison SF. A thermosensory pathway mediating heat-defense responses. *Proc Natl Acad Sci U S A* 2010; **107**: 8848–8853.

3 Tan CL, Knight ZA. Regulation of Body Temperature by the Nervous System. *Neuron* 2018; **98**: 31–48.

4 Dimicco JA, Zaretsky D V. The dorsomedial hypothalamus: a new player in thermoregulation. *Am J Physiol Regul Integr Comp Physiol* 2007; **292**: R47-63.

5 Bratincsák A, Palkovits M. Activation of brain areas in rat following warm and cold ambient exposure. *Neuroscience* 2004; **127**: 385–397.

6 Busto R, Globus MY, Dietrich WD, Martinez E, Valdés I, Ginsberg MD. Effect of mild hypothermia on ischemia-induced release of neurotransmitters and free fatty acids in rat brain. *Stroke* 1989; **20**: 904–910.

7 Adachi M, Sohma O, Tsuneishi S, Takada S, Nakamura H. Combination effect of systemic hypothermia and caspase inhibitor administration against hypoxic-ischemic brain damage in neonatal rats. *Pediatr Res* 2001; **50**: 590–595.

8 Jiang JY, Lyeth BG, Kapasi MZ, Jenkins LW, Povlishock JT. Moderate hypothermia reduces blood-brain barrier disruption following traumatic brain injury in the rat. *Acta Neuropathol* 1992; **84**: 495–500.

9 Baumann E, Preston E, Slinn J, Stanimirovic D. Post-ischemic hypothermia attenuates loss of the vascular basement membrane proteins, agrin and SPARC, and the blood-brain barrier disruption after global cerebral ischemia. *Brain Res* 2009; **1269**: 185–197.

10 Katz LM, Young AS, Frank JE, Wang Y, Park K. Regulated hypothermia reduces brain oxidative stress after hypoxic-ischemia. *Brain Res* 2004; **1017**: 85–91.

11 Stefanutti G, Pierro A, Vinardi S, Spitz L, Eaton S. Moderate hypothermia protects

ARTICLE IN PRESS

against systemic oxidative stress in a rat model of intestinal ischemia and reperfusion injury. *Shock* 2005; **24**: 159–164.

12 Wu L, Wu D, Yang T, Xu J, Chen J, Wang L *et al.* Hypothermic neuroprotection against acute ischemic stroke: The 2019 update. *J Cereb blood flow Metab Off J Int Soc Cereb Blood Flow Metab* 2020; **40**: 461–481.

13 Feigin VL, Brainin M, Norrving B, Martins S, Sacco RL, Hacke W *et al.* World Stroke Organization (WSO): Global Stroke Fact Sheet 2022. *Int J stroke Off J Int Stroke Soc* 2022; **17**: 18–29.

14 Katan M, Luft A. Global Burden of Stroke. *Semin Neurol* 2018; **38**: 208–211.

15 Chen X, Zheng J, Wang J, Wang H, Shi H, Jiang H *et al.* Global burden and cross-country inequalities in stroke and subtypes attributable to diet from 1990 to 2019. *BMC Public Health* 2024; **24**: 1813.

16 Lyden PD, Krieger D, Yenari M, Dietrich WD. Therapeutic hypothermia for acute stroke. *Int J stroke Off J Int Stroke Soc* 2006; **1**: 9–19.

17 Wu T-C, Grotta JC. Hypothermia for acute ischaemic stroke. *Lancet Neurol* 2013; **12**: 275–284.

18 You JS, Kim JY, Yenari MA. Therapeutic hypothermia for stroke: Unique challenges at the bedside. *Front Neurol* 2022; **13**: 951586.

19 Huckabee HC, Craig PL, Williams JM. Near drowning in frigid water: a case study of a 31-year-old woman. *J Int Neuropsychol Soc* 1996; **2**: 256–260.

20 Siebke H, Rod T, Breivik H, Link B. Survival after 40 minutes; submersion without cerebral sequeae. *Lancet (London, England)* 1975; **1**: 1275–1277.

21 Polderman KH. Application of therapeutic hypothermia in the ICU: opportunities and pitfalls of a promising treatment modality. Part 1: Indications and evidence. *Intensive Care Med* 2004; **30**: 556–575.

22 Binda DD, Baker MB, Varghese S, Wang J, Badenes R, Bilotta F *et al.* Targeted

ARTICLE IN PRESS

Temperature Management for Patients with Acute Ischemic Stroke: A Literature Review. *J Clin Med* 2024; **13**. doi:10.3390/jcm13020586.

23 Boubes K, Batlle D, Tang T, Torres J, Paul V, Abdul HM *et al.* Serum potassium changes during hypothermia and rewarming: a case series and hypothesis on the mechanism. *Clin Kidney J* 2023; **16**: 827–834.

24 Ellis RJ, Mavroudis C, Gardner C, Turley K, Ullyot D, Ebert PA. Relationship between atrioventricular arrhythmias and the concentration of K+ ion in cardioplegic solution. *J Thorac Cardiovasc Surg* 1980; **80**: 517–526.

25 Nielsen AKW, Jeppesen AN, Kirkegaard H, Hvas A-M. Changes in coagulation during therapeutic hypothermia in cardiac arrest patients. *Resuscitation* 2016; **98**: 85–90.

26 Zhao Z-D, Yang WZ, Gao C, Fu X, Zhang W, Zhou Q *et al.* A hypothalamic circuit that controls body temperature. *Proc Natl Acad Sci U S A* 2017; **114**: 2042–2047.

27 Mathews LC, Gray JT, Gallagher MR, Snyder RO. Recombinant adeno-associated viral vector production using stable packaging and producer cell lines. *Methods Enzymol* 2002; **346**: 393–413.

28 Atasoy D, Betley JN, Su HH, Sternson SM. Deconstruction of a neural circuit for hunger. *Nature* 2012; **488**: 172–177.

29 Dilsiz P, Aklan I, Sayar Atasoy N, Yavuz Y, Filiz G, Koksalar F *et al.* MCH Neuron Activity Is Sufficient for Reward and Reinforces Feeding. *Neuroendocrinology* 2020; **110**. doi:10.1159/000501234.

30 Aklan I, Sayar Atasoy N, Yavuz Y, Ates T, Coban I, Koksalar F *et al.* NTS Catecholamine Neurons Mediate Hypoglycemic Hunger via Medial Hypothalamic Feeding Pathways. *Cell Metab* 2020; **31**. doi:10.1016/j.cmet.2019.11.016.

31 Dilsiz P, Aklan I, Coban I, Oncul M, Alkan F, Celik E *et al.* Melanin Concentrating Hormone Neurons Regulate Reward Seeking Independent of Post-Ingestive Actions. *Neuroendocrinology* 2018; **107 MA**-: 8.

ARTICLE IN PRESS

32 Balçıkanlı Z, Culha I, Dilsiz P, Aydin MS, Ates N, Beker MC *et al.* Lithium promotes long-term neurological recovery after spinal cord injury in mice by enhancing neuronal survival, gray and white matter remodeling, and long-distance axonal regeneration. *Front Cell Neurosci* 2022; **16**: 1012523.

33 Martins HC, Gilardi C, Sungur AÖ, Winterer J, Pelzl MA, Bicker S *et al.* Bipolar-associated miR-499-5p controls neuroplasticity by downregulating the Cav1.2 subunit CACNB2. *EMBO Rep* 2022; **23**: e54420.

34 Beker MC, Aydinli FI, Caglayan AB, Beker M, Baygul O, Caglayan A *et al.* Age-Associated Resilience Against Ischemic Injury in Mice Exposed to Transient Middle Cerebral Artery Occlusion. *Mol Neurobiol* 2023; **60**: 4359–4372.

35 Beker MC, Caglayan AB, Kelestemur T, Caglayan B, Yalcin E, Yulug B *et al.* Effects of normobaric oxygen and melatonin on reperfusion injury: role of cerebral microcirculation. *Oncotarget* 2015; **6**: 30604–30614.

36 Kilic U, Caglayan AB, Beker MC, Gunal MY, Caglayan B, Yalcin E *et al.* Particular phosphorylation of PI3K/Akt on Thr308 via PDK-1 and PTEN mediates melatonin's neuroprotective activity after focal cerebral ischemia in mice. *Redox Biol* 2017; **12**: 657–665.

37 Ates N, Caglayan A, Balcikanli Z, Sertel E, Beker MC, Dilsiz P *et al.* Phosphorylation of PI3K/Akt at Thr308, but not phosphorylation of MAPK kinase, mediates lithium-induced neuroprotection against cerebral ischemia in mice. *Exp Neurol* 2022; **351**: 113996.

38 Bacigaluppi M, Pluchino S, Peruzzotti-Jametti L, Kilic E, Kilic U, Salani G *et al.* Delayed post-ischaemic neuroprotection following systemic neural stem cell transplantation involves multiple mechanisms. *Brain* 2009; **132**: 2239–2251.

39 Hermann DM, Kilic E, Hata R, Hossmann KA, Mies G. Relationship between metabolic dysfunctions, gene responses and delayed cell death after mild focal cerebral ischemia in mice. *Neuroscience* 2001; **104**: 947–955.

ARTICLE IN PRESS

ARTICLE IN PRESS

40 Sofroniew M V. Astrocyte barriers to neurotoxic inflammation. *Nat Rev Neurosci* 2015; **16**: 249–263.

41 Li L, Zhou J, Han L, Wu X, Shi Y, Cui W *et al.* The Specific Role of Reactive Astrocytes in Stroke. *Front Cell Neurosci* 2022; **16**: 850866.

42 Shen X-Y, Gao Z-K, Han Y, Yuan M, Guo Y-S, Bi X. Activation and Role of Astrocytes in Ischemic Stroke. *Front Cell Neurosci* 2021; **15**: 755955.

43 Dzyubenko E, Hermann DM. Role of glia and extracellular matrix in controlling neuroplasticity in the central nervous system. *Semin Immunopathol* 2023; **45**: 377–387.

44 Borbor M, Yin D, Brockmeier U, Wang C, Doeckel M, Pillath-Eilers M *et al.* Neurotoxicity of ischemic astrocytes involves STAT3-mediated metabolic switching and depends on glycogen usage. *Glia* 2023; **71**: 1553–1569.

45 Gao J, Zhao Y, Li T, Gan X, Yu H. The Role of PKM2 in the Regulation of Mitochondrial Function: Focus on Mitochondrial Metabolism, Oxidative Stress, Dynamic, and Apoptosis. PKM2 in Mitochondrial Function. *Oxid Med Cell Longev* 2022; **2022**: 7702681.

46 Ren J, Gao J, Yao X, Wang X, Kong X, Lin T *et al.* Bilateral transcranial direct-current stimulation confers neuroprotection through suppression of PKM2 after mouse cerebral ischemia injury. *Brain Res* 2025; **1849**: 149353.

47 Ouyang Y-B, Giffard RG. Bcl-XL maintains mitochondrial function in murine astrocytes deprived of glucose. *J Cereb blood flow Metab Off J Int Soc Cereb Blood Flow Metab* 2003; **23**: 275–279.

48 Zweifler RM, Sessler DI. Thermoregulatory vasococonstriction and shivering impede therapeutic hypothermia in acute ischemic stroke patients. *J stroke Cerebrovasc Dis Off J Natl Stroke Assoc* 1996; **6**: 100–103.

49 Liu B, Luo W, Zhang Y, Li H, Zhu N, Huang D *et al.* Involvement of cyclo-oxygenase-1-mediated prostacyclin synthesis in the vasoconstrictor activity evoked by ACh in mouse arteries. *Exp Physiol* 2012; **97**: 277–289.

ARTICLE IN PRESS

ARTICLE IN PRESS

50 Haynes WG, Webb DJ. Contribution of endogenous generation of endothelin-1 to basal vascular tone. *Lancet (London, England)* 1994; **344**: 852–854.

51 Gonzalez FF, Monsell SE, Cornet M-C, Glass H, Wisnowski J, Mathur A *et al.* Perinatal arterial ischemic stroke diagnosed in infants receiving therapeutic hypothermia for hypoxic-ischemic encephalopathy. *Pediatr Res* 2024. doi:10.1038/s41390-024-03531-7.

52 Hägerdal M, Harp J, Nilsson L, Siesjö BK. The effect of induced hypothermia upon oxygen consumption in the rat brain. *J Neurochem* 1975; **24**: 311–316.

53 Ávila-Gómez P, Vieites-Prado A, Dopico-López A, Bashir S, Fernández-Susavila H, Gubern C *et al.* Cold stress protein RBM3 responds to hypothermia and is associated with good stroke outcome. *Brain Commun* 2020; **2**: fcaa078.

54 Chip S, Zelmer A, Ogunshola OO, Felderhoff-Mueser U, Nitsch C, Bührer C *et al.* The RNA-binding protein RBM3 is involved in hypothermia induced neuroprotection. *Neurobiol Dis* 2011; **43**: 388–396.

55 Xu Y, Duan Y, Xu S, He X, Guo J, Shi J *et al.* Mild hypothermia therapy attenuates early BBB leakage in acute ischemic stroke. *J Cereb blood flow Metab Off J Int Soc Cereb Blood Flow Metab* 2025; **45**: 292–305.

56 Hong JM, Lee JS, Song H-J, Jeong HS, Choi HA, Lee K. Therapeutic hypothermia after recanalization in patients with acute ischemic stroke. *Stroke* 2014; **45**: 134–140.

57 Hemmen TM, Raman R, Guluma KZ, Meyer BC, Gomes JA, Cruz-Flores S *et al.* Intravenous thrombolysis plus hypothermia for acute treatment of ischemic stroke (ICTuS-L): final results. *Stroke* 2010; **41**: 2265–2270.

58 Schwab S, Schwarz S, Spranger M, Keller E, Bertram M, Hacke W. Moderate hypothermia in the treatment of patients with severe middle cerebral artery infarction. *Stroke* 1998; **29**: 2461–2466.

59 Tan CL, Cooke EK, Leib DE, Lin Y-C, Daly GE, Zimmerman CA *et al.* Warm-Sensitive Neurons that Control Body Temperature. *Cell* 2016; **167**: 47-59.e15.

ARTICLE IN PRESS

60 Wang Y, Song Y, Tong L, Wang L, Cao J, Qin G *et al.* GABAergic neurons in the dorsomedial hypothalamus regulate states of consciousness in sevoflurane anesthesia. *iScience* 2023; **26**: 105913.

61 Hemingway A, Forgave P, Birzis L. Shivering suppression by hypothalamic stimulation. *J Neurophysiol* 1954; **17**: 375–386.

62 Magoun HW, Harrison F, Brobeck JR, Ranson SW. Activation of heat loss mechanisms by local heating of the brain. *J Neurophysiol* 1938; **1**: 101–114.

63 Boulant JA. Role of the preoptic-anterior hypothalamus in thermoregulation and fever. *Clin Infect Dis an Off Publ Infect Dis Soc Am* 2000; **31 Suppl 5**: S157-61.

64 Hori T, Nakashima T, Koga H, Kiyohara T, Inoue T. Convergence of thermal, osmotic and cardiovascular signals on preoptic and anterior hypothalamic neurons in the rat. *Brain Res Bull* 1988; **20**: 879–885.

65 Thompson RH, Canteras NS, Swanson LW. Organization of projections from the dorsomedial nucleus of the hypothalamus: a PHA-L study in the rat. *J Comp Neurol* 1996; **376**: 143–173.

66 Nakamura Y, Nakamura K, Matsumura K, Kobayashi S, Kaneko T, Morrison SF. Direct pyrogenic input from prostaglandin EP3 receptor-expressing preoptic neurons to the dorsomedial hypothalamus. *Eur J Neurosci* 2005; **22**: 3137–3146.

67 Chen XM, Hosono T, Yoda T, Fukuda Y, Kanosue K. Efferent projection from the preoptic area for the control of non-shivering thermogenesis in rats. *J Physiol* 1998; **512 (Pt 3**: 883–892.

68 Monge-Roffarello B, Labbe SM, Lenglos C, Caron A, Lanfray D, Samson P *et al.* The medial preoptic nucleus as a site of the thermogenic and metabolic actions of melanotan II in male rats. *Am J Physiol Regul Integr Comp Physiol* 2014; **307**: R158-66.

69 de Menezes RCA, Zaretsky D V, Fontes MAP, DiMicco JA. Microinjection of muscimol into caudal periaqueductal gray lowers body temperature and attenuates increases in

ARTICLE IN PRESS

temperature and activity evoked from the dorsomedial hypothalamus. *Brain Res* 2006; **1092**: 129–137.

70 DiMicco JA, Abshire VM. Evidence for GABAergic inhibition of a hypothalamic sympathoexcitatory mechanism in anesthetized rats. *Brain Res* 1987; **402**: 1–10.

71 Liddelow SA, Guttenplan KA, Clarke LE, Bennett FC, Bohlen CJ, Schirmer L *et al.* Neurotoxic reactive astrocytes are induced by activated microglia. *Nature* 2017; **541**: 481–487.

72 Keatinge WR. The effect of general chilling on the vasodilator response to cold. *J Physiol* 1957; **139**: 497–507.

73 Aronowski J, Strong R, Grotta JC. Reperfusion injury: demonstration of brain damage produced by reperfusion after transient focal ischemia in rats. *J Cereb blood flow Metab Off J Int Soc Cereb Blood Flow Metab* 1997; **17**: 1048–1056.

74 Yang GY, Betz AL. Reperfusion-induced injury to the blood-brain barrier after middle cerebral artery occlusion in rats. *Stroke* 1994; **25**: 1655–1658.

75 Luber B, Davis SW, Deng Z-D, Murphy D, Martella A, Peterchev A V *et al.* Using diffusion tensor imaging to effectively target TMS to deep brain structures. *Neuroimage* 2022; **249**: 118863.

ARTICLE IN PRESS

ARTICLE IN PRESS

Figure legends:

Fig. 1: Schematic illustration of the experimental design. Hypothermia was induced by chemogenetic silencing of dorsomedial hypothalamic DMH^{VGAT} neurons by clozapine (CLZ) or optogenetic activation of the GABAergic ventrolateral preoptic area $vlPOA^{VGAT}$ → DMH pathway by 473 nm laser light. Consequences for brain tissue survival and ischemic injury were investigated.

Fig. 2: Chemogenetic silencing of GABAergic DMH^{VGAT} neurons induces hypothermia. (A) Cartoon illustrating chemogenetic DMH^{VGAT} neuron silencing as a strategy for inducing hypothermia. **(B)** An AAV vector with double-floxed inverted open-reading frame (DIO) hM4D(Gi) was bilaterally injected into the DMH of *Vgat-cre* mice, resulting in selective expression of the DREADD hM4D(Gi) in GABAergic DMH^{VGAT} neurons. Representative photomicrograph showing $DMH^{VGAT:hM4D}$ expression. Scale bar: 500 μm. **(C)** Core body temperature measurements of $DMH^{VGAT:hM4D}$ and $DMH^{VGAT:GFP}$ mice (n=9 each) after intraperitoneal (i.p.) clozapine (CLZ) delivery at t=0 (left panel). Maximum body temperature changes were observed at t=90 min. **(D)** Infrared thermography demonstrating decreased body temperature and tail vasoconstriction upon DMH^{VGAT} neuron inhibition. Open field tests revealed that **(E)** average speed, **(F)** time mobile and **(G)** total distance covered decreased upon CLZ injection in $DMH^{VGAT:hM4D}$ compared to $DMH^{VGAT:GFP}$ mice (n=9 each). **(H)** Cumulative heatmaps depicting time spent in different locations of the open field chamber during DMH^{VGAT} silencing. Note that DMH^{VGAT} silencing decreased overall animal motor activity. Data are mean ± SEM values. *p < 0.05, **p < 0.01, ***p < 0.001.

Fig. 3: Chemogenetic DMH^{VGAT} silencing decreases infarct volume, neurological deficits and brain edema. (A) Cartoon showing the 90 min MCAo model followed by 24 hours reperfusion that results in focal infarcts of the striatum and overlying cortex. Effect of CLZ-induced DMH^{VGAT}

silencing on **(B)** infarct volume and **(C)** brain swelling examined by cresyl violet staining and **(D)** BBB leakage measured by serum IgG extravasation analysis and **(E)** neurological deficits evaluated by the Bederson score in $DMH^{VGAT:hM4D}$ DREADD mice (n=8) compared to $DMH^{VGAT:GFP}$ non-DREADD control mice (n=6). Representative cresyl violet and IgG extravasation images are shown. Scale bars: 2 mm. Data are mean ± SEM values. *p < 0.05, **p < 0.01.

Fig. 4: DMH^{VGAT} silencing increases post-ischemic neuronal survival and preserves the homeostatic astrocyte state. (A) Cartoon depicting the 30 min MCAo model followed by 72 hours reperfusion that results in disseminate neuronal injury in the striatum. **(B)** Representative photomicrographs showing the effect of CLZ-induced DMH^{VGAT} silencing on neuronal survival and astroglial responses evaluated by NeuN and GFAP immunolabeling. Quantification of **(C)** neuronal survival and **(D)** astroglial GFAP immunoreactivity in $DMH^{VGAT:hM4D}$ mice (n=10) compared to $DMH^{VGAT:GFP}$ control mice (n=9). **(E)** Representative photomicrographs and **(F, G)** quantification of PKM2 expression, a marker of the detrimental “neurotoxic” astrocyte state, in $GFAP^{+}$ astrocytes and $GFAP^{-}$ cells (cell nuclei counterstained with DAPI). Note that CLZ-induced DMH^{VGAT} silencing reduced astrocytic PKM2 expression, indicative that astrocytes retained their homeostatic phenotype (n=17-18 ROIs in n=4 mice per group). Scale bars: 50 µm. Data are mean ± SEM values. *p < 0.05, ***p < 0.001.

Fig. 5: DMH^{VGAT} silencing decreases post-ischemic reperfusion and reperfusion injury. (A) Experimental timeline and areas of interest for analysis of laser speckle images after chemogenetic DMH^{VGAT} silencing. **(B)** Representative laser speckle images in response to CLZ in $DMH^{VGAT:hM4D}$ and $DMH^{VGAT:GFP}$ mice at baseline, during MCAo and at 30- and 60-min following reperfusion. Quantitative analysis of regional CBF in **(C)** the ischemic core and **(D)** the penumbra showing decreased reperfusion after CLZ-induced DMH^{VGAT} silencing (n=3 each). **(E)** Effect of chemogenetic DMH^{VGAT} silencing on post-ischemic reperfusion injury in the striatum assessed by

TUNEL in $DMH^{VGAT:hM4D}$ (n=10) and $DMH^{VGAT:GFP}$ control mice (n=9). In **(F)**, representative TUNEL stainings exhibiting DNA-fragmented cells are shown. Note the strong reduction of $TUNEL^{+}$ cells in the striatum of $DMH^{VGAT:hM4D}$ compared to $DMH^{VGAT:GFP}$ control mice. Scale bars: 1 mm (overview images)/ 250 µm (magnifications). Data are mean ± SEM values. *p < 0.05.

Fig. 6: Optogenetic activation of GABAergic $vlPOA^{VGAT}$ → DMH pathway induces hypothermia. (A) Cartoon illustrating optogenetic activation of the $vlPOA^{VGAT}$ → DMH pathway as a strategy for inducing hypothermia. An AAV vector with double-floxed inverted open-reading frame (DIO) hChR2-eYFP was unilaterally injected into the vlPOA of *Vgat-cre* mice, resulting in selective expression of hChR2-eYFP in GABAergic vlPOA neurons and DMH-projecting nerve fibers, as shown in representative microscopic images. Representative photomicrograph showing fiber tip (F.T.) placement above the DMH. Scale: 500 µm. Optical stimulation was performed with 473 nm laser light. **(B)** Photomicrograph (left) and quantification (right) of c-Fos expression in the DMH of ChR2-expressing (n=36) or GFP-expressing (n=4) mice during 10 Hz photostimulation. **(C)** Effect of optical stimulation from the fiber tip on core body temperature in $vlPOA^{VGAT:ChR2}$ mice (n=6) compared to $vlPOA^{VGAT:GFP}$ control mice (n=8). Maximum body temperature changes were observed at t=60 min. **(D)** Infrared thermography demonstrating decreased body temperature and tail vasoconstriction upon optical stimulation of $vlPOA^{VGAT}$ nerve terminals in the DMH. Scale bar: 50 µm. Data are mean ± SEM values. ***p < 0.001.

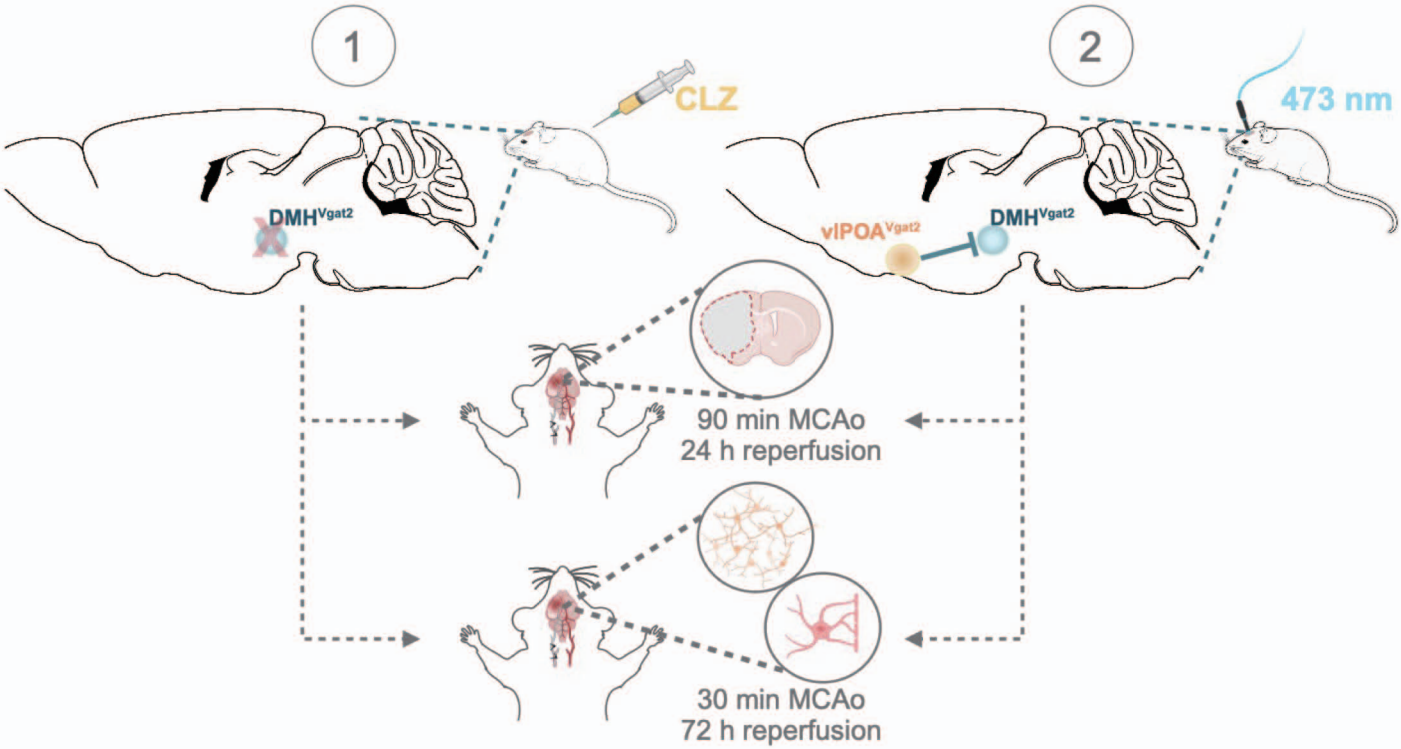
Fig. 7: Activation of $vlPOA^{VGAT}$ → DMH pathway reduces ischemic infarct volume, brain edema and cell injury. Effect of optogenetic activation of the $vlPOA^{VGAT}$ → DMH pathway on **(A)** infarct volume and **(B)** brain edema examined by cresyl violet staining as well as **(C)** BBB leakage assessed by IgG extravasation analysis in optogenetically stimulated $vlPOA^{VGAT:ChR2}$ mice (n=6) compared to $vlPOA^{VGAT:GFP}$ control mice (n=8) exposed to 90 min MCAo followed by 24 hours reperfusion. Representative cresyl violet and IgG stainings are shown. Scale bars: 2 mm. **(D)**

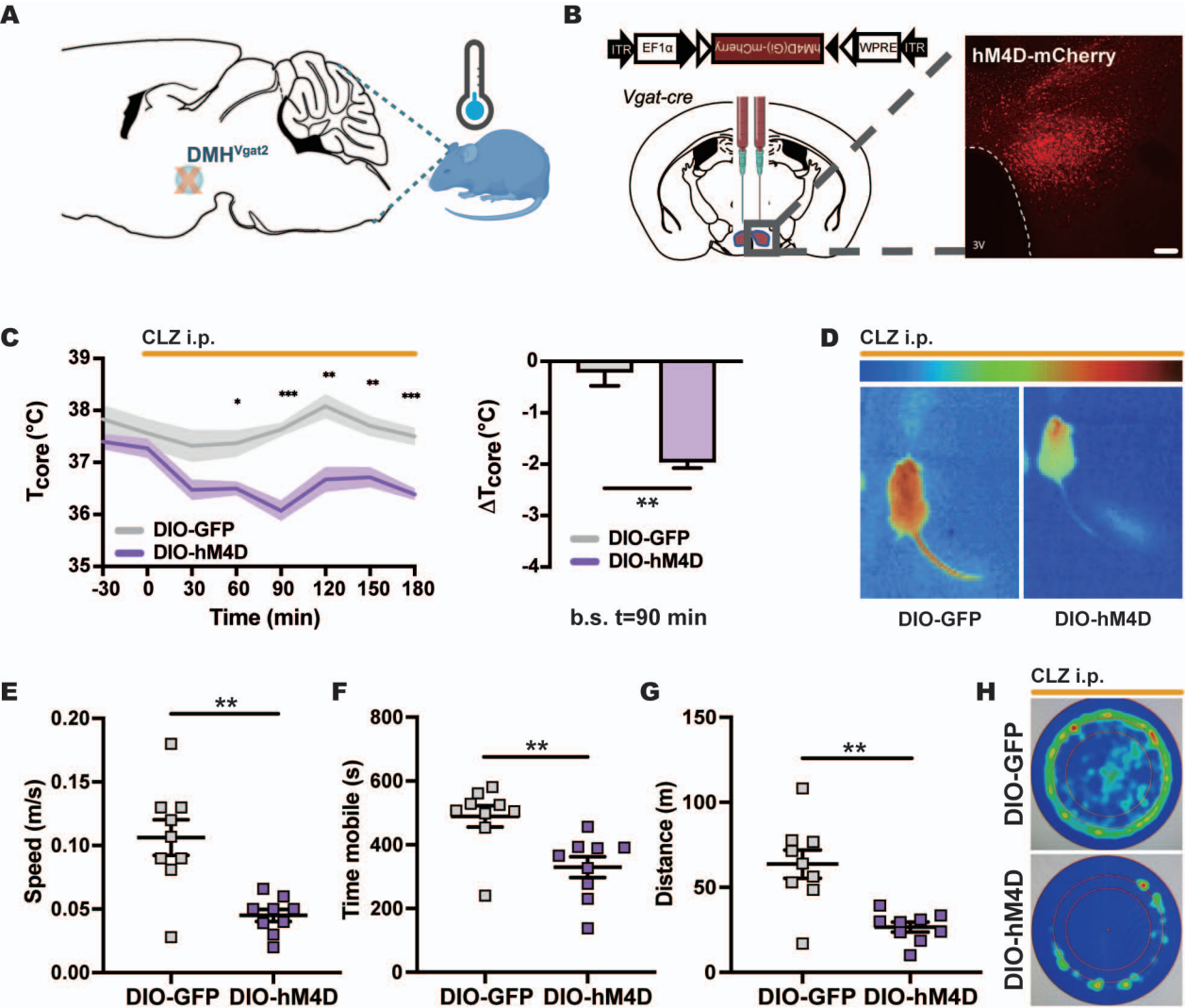
ARTICLE IN PRESS

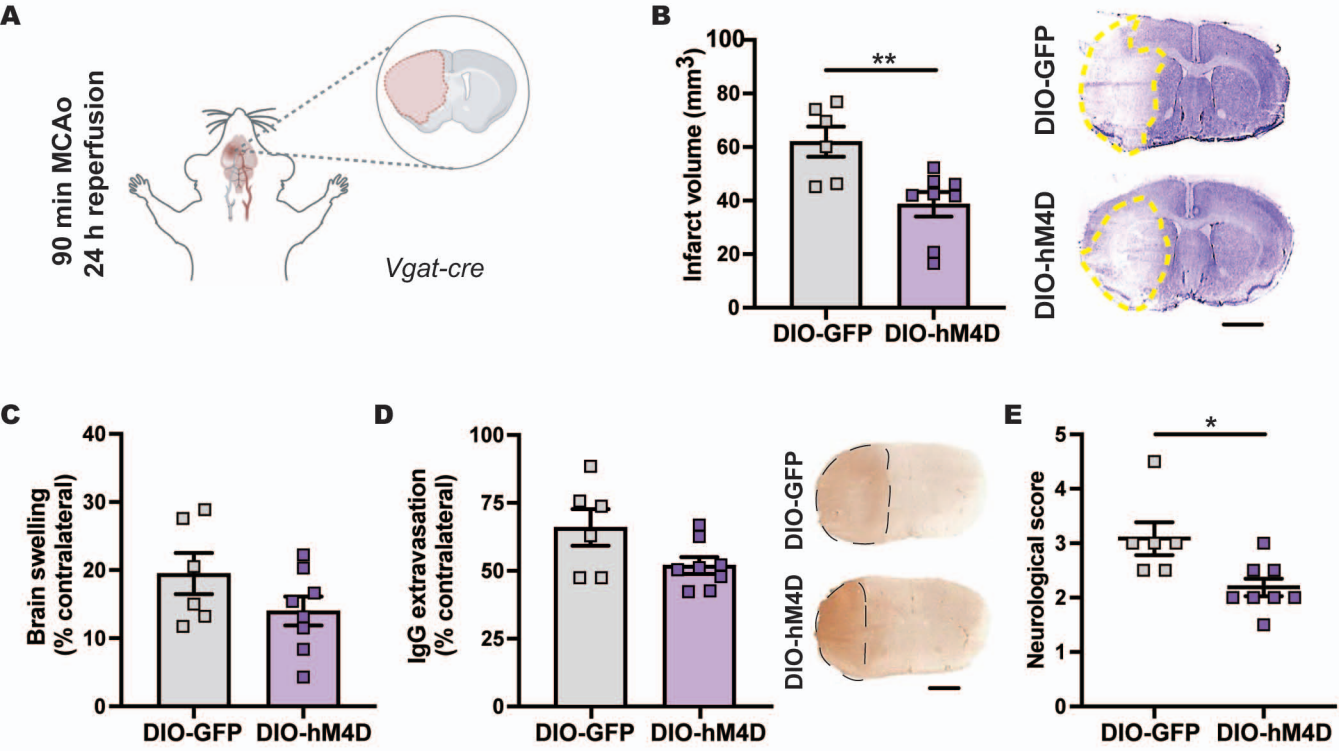
Effect of optogenetic vlPOA^{VGAT} → DMH projection activation on post-ischemic reperfusion injury in the striatum assessed by TUNEL in vlPOA$^{VGAT:ChR2}$ and vlPOA$^{VGAT:GFP}$ mice (n=7 each) exposed to 30 min MCAo followed by 72 hours reperfusion. In **(E)**, representative TUNEL stainings exhibiting DNA-fragmented cells are shown. Note the strong reduction of TUNEL^{+} cells in the striatum of vlPOA$^{VGAT:ChR2}$ compared with vlPOA$^{VGAT:GFP}$ control mice. Scale bars: 1 mm (overview images)/ 250 µm (magnifications). Data are mean ± SEM values. *p < 0.05, **p < 0.01.

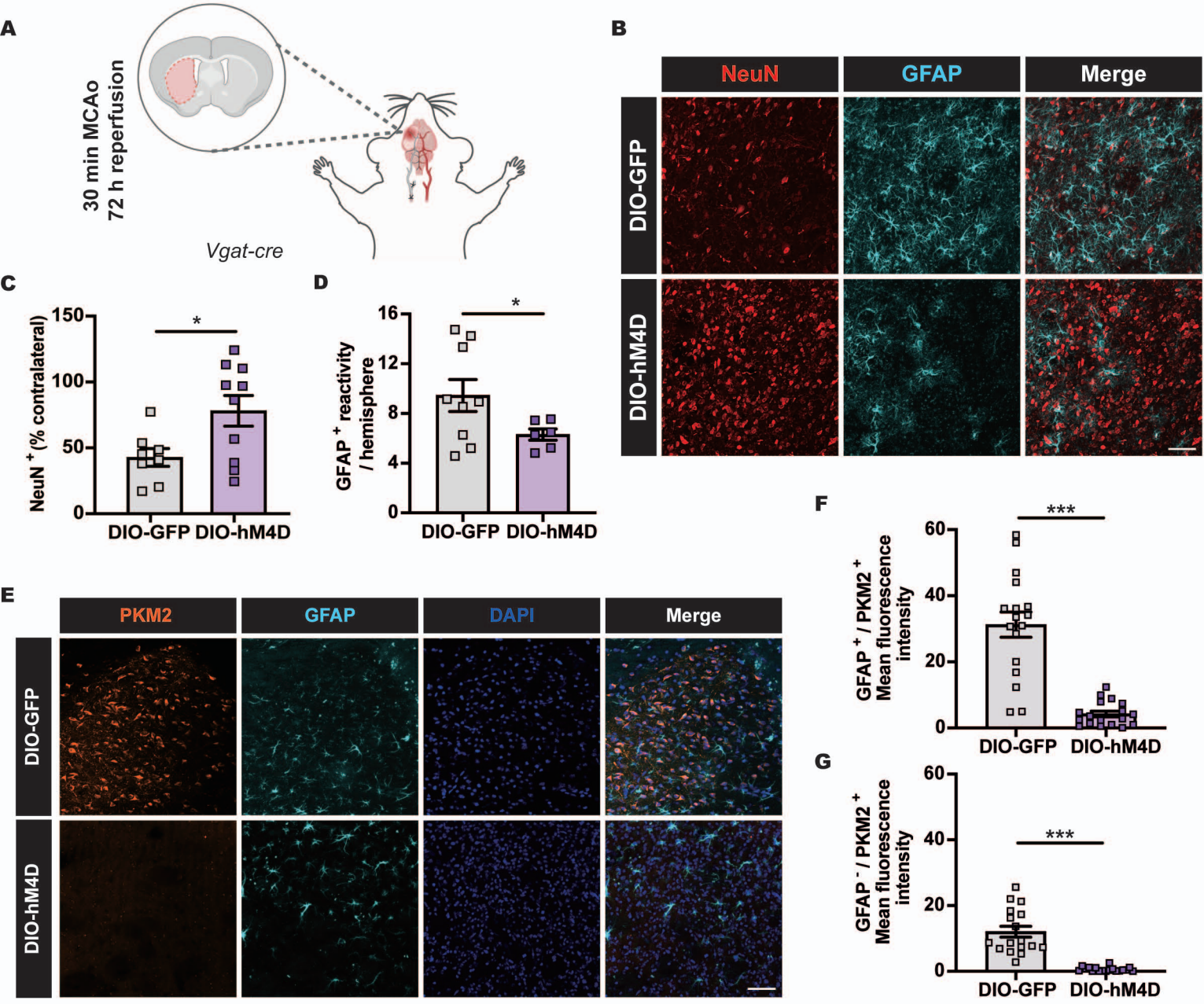
Fig. 8: vlPOA^{VGAT} → DMH pathway activation increases post-ischemic neuronal survival and preserves astrocytic homeostasis. (A) Representative photomicrographs showing the effect of optogenetic vlPOA^{VGAT} → DMH pathway activation on neuronal survival and astroglial responses evaluated by NeuN and GFAP immunolabeling in mice exposed to 30 min MCAo followed by 72 hours reperfusion. Quantification of **(B)** neuronal survival and **(C)** astroglial GFAP immunoreactivity in stimulated vlPOA$^{VGAT:ChR2}$ mice (n=7) compared to vlPOA$^{VGAT:GFP}$ control mice (n=7). **(D)** Representative photomicrographs and **(E, F)** quantification of PKM2 immunoreactivity, a marker of “neurotoxic” astrocytes, in GFAP^{+} astrocytes and GFAP^{-} cells (nuclei counterstained with DAPI). Note that optogenetic vlPOA^{VGAT} → DMH activation reduced PKM2 expression, indicative that astrocytes retained their homeostatic state (n=17-18 ROIs in n=4 mice per group). Scale bars: 50 µm. Data are mean ± SEM values. **p < 0.01, ***p < 0.001.

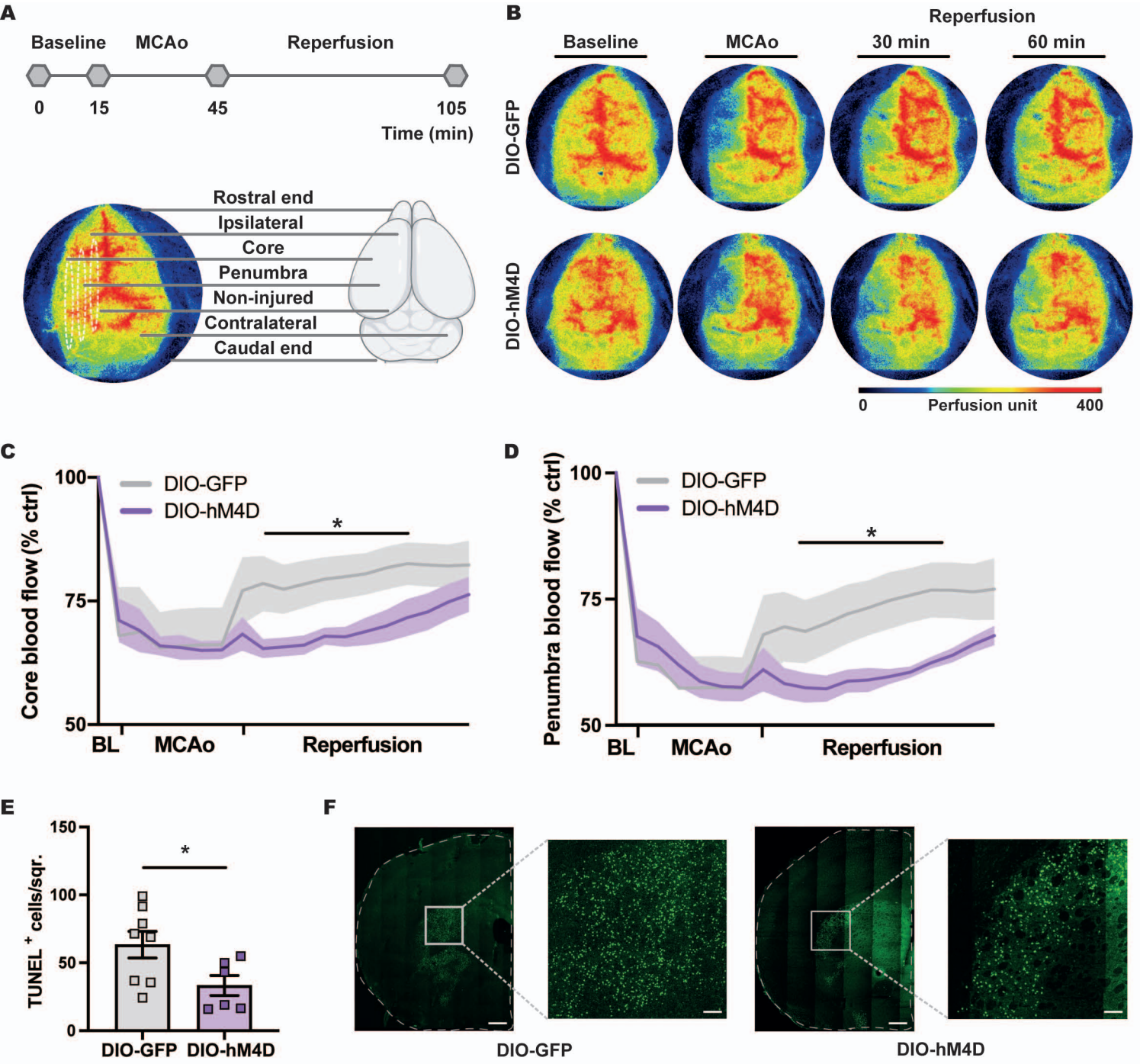
Thumbnail: Graphical abstract: GABAergic vlPOA^{VGAT} → DMH pathway activation lowers body core temperature, limits post-ischemic infarct volume and enhances neuronal survival by reducing reperfusion damage. Hypothermia was chemogenetically or optogenetically induced in mice exposed to 90 or 30 min middle cerebral artery occlusion (MCAo). Structural and functional consequences of GABAergic vlPOA^{VGAT} → DMH pathway modulation were assessed.

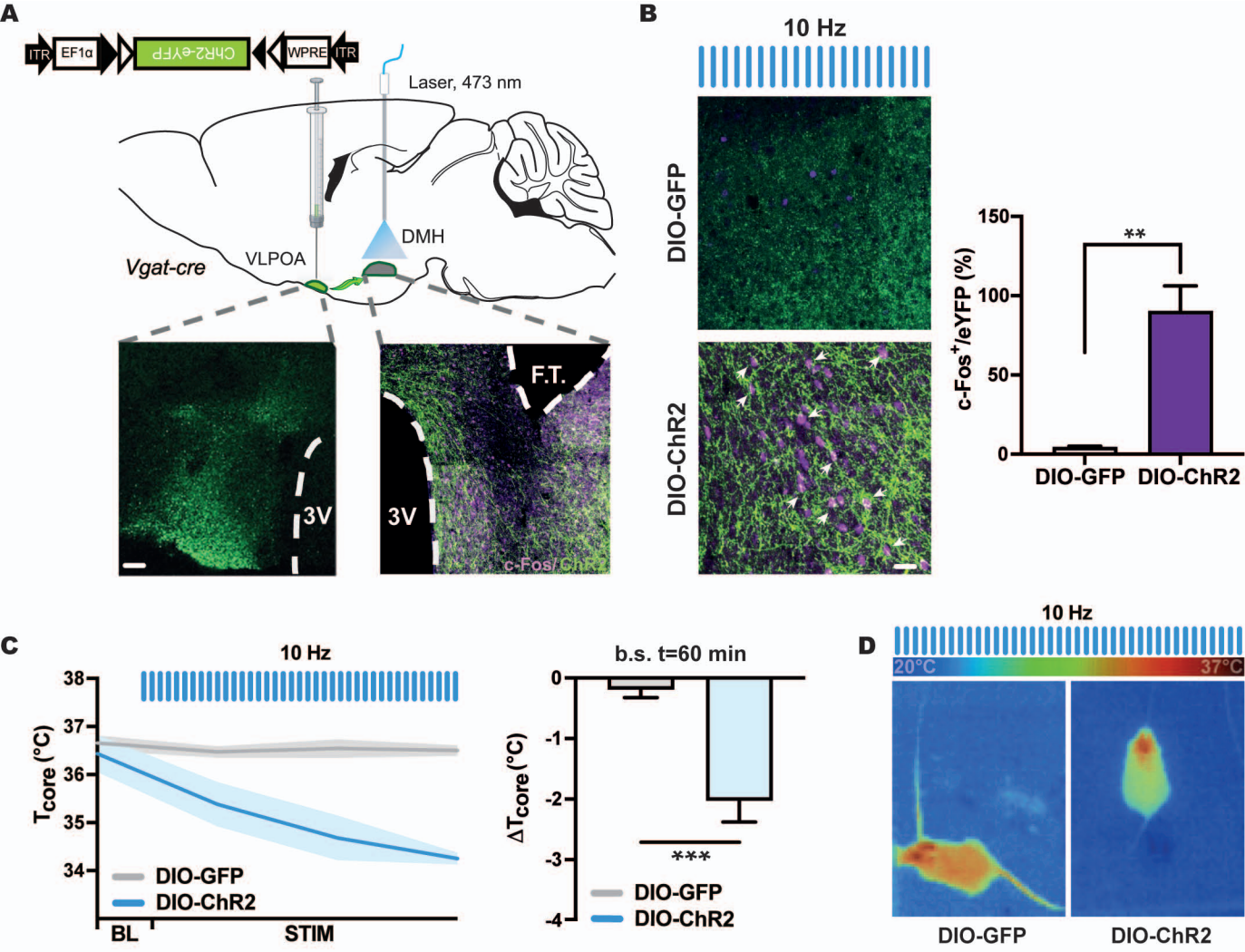

1
CLZ
DMH Vgat2
2
473 nm
vlPOA Vgat2
DMH Vgat2
90 min MCAo
24 h reperfusion
30 min MCAo
72 h reperfusion

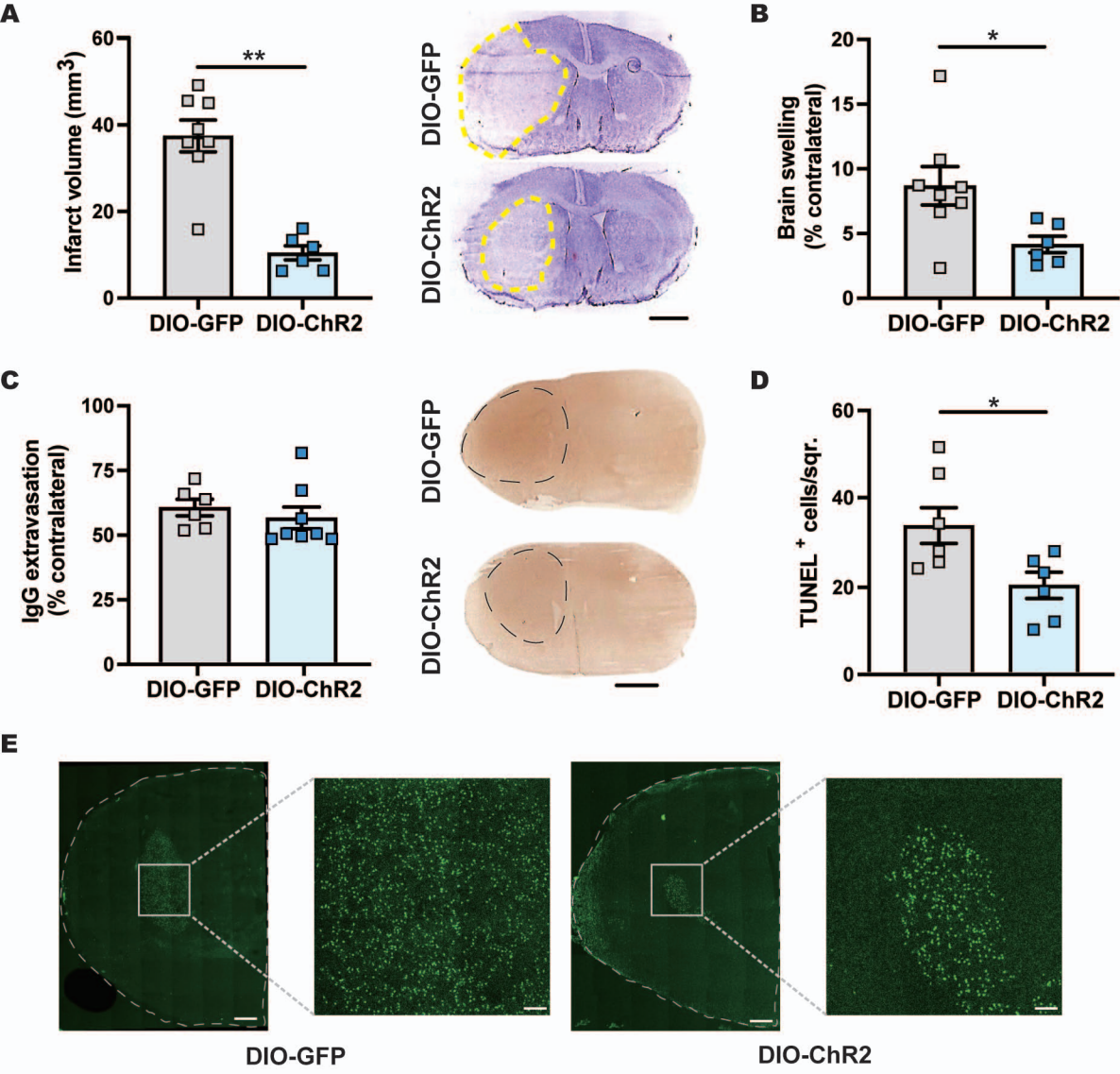

A
DMH Vgat2
B
ITR
EF1α
hM4D(Gi)-mCherry
WPRE
ITR
Vgat-cre
hM4D-mCherry
3V
C
CLZ i.p.
Tcore (°C)
Time (min)
DIO-GFP
DIO-hM4D
ΔTcore (°C)
b.s. t=90 min
D
CLZ i.p.
DIO-GFP
DIO-hM4D
E
Speed (m/s)
F
Time mobile (s)
G
Distance (m)
H
CLZ i.p.
DIO-GFP
DIO-hM4D

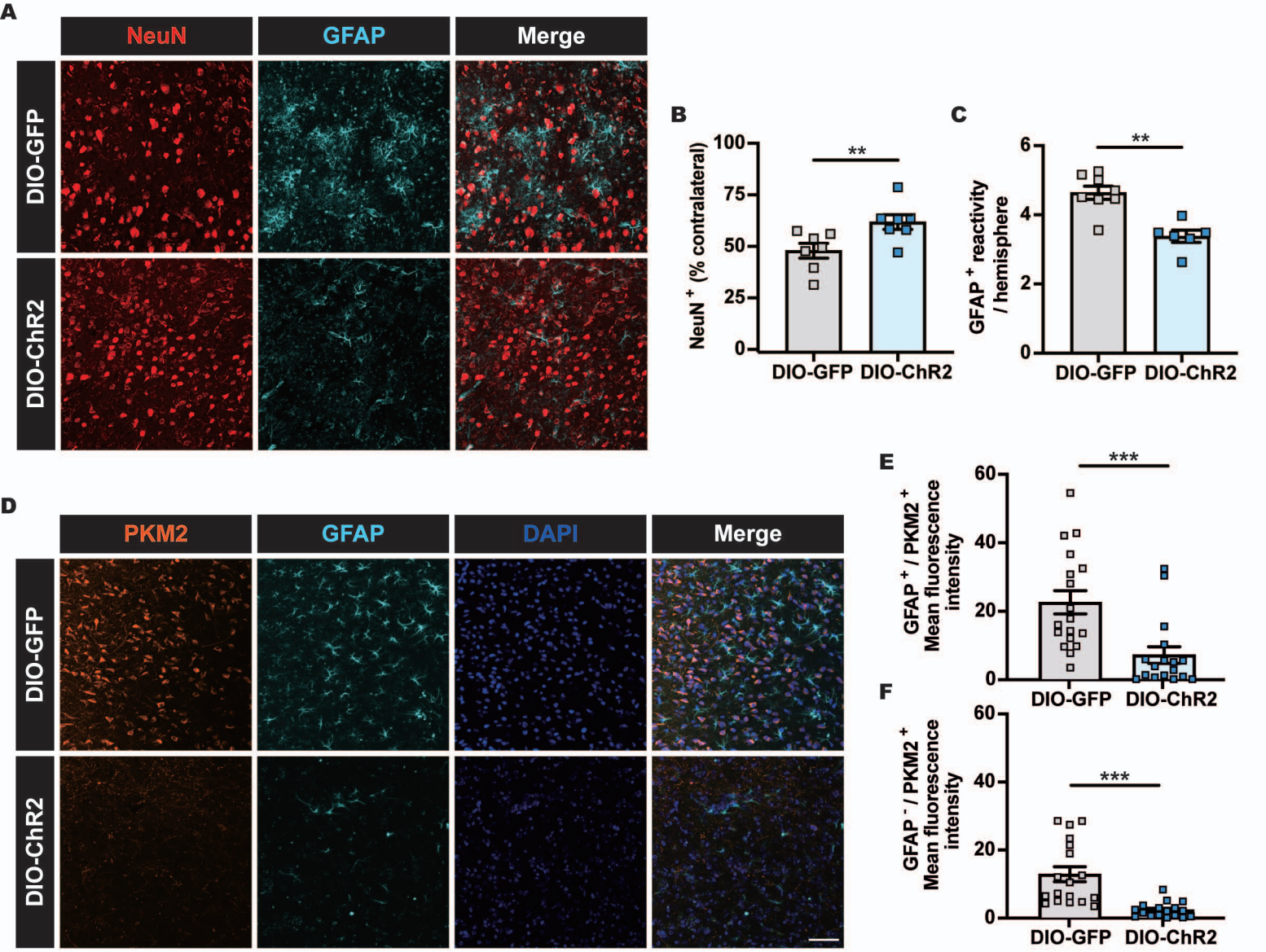

A
90 min MCAo
24 h reperfusion
Vgat-cre
B
Infarct volume (mm3)
100
80
60
40
20
0
**
DIO-GFP
DIO-hM4D
DIO-GFP
DIO-hM4D
C
Brain swelling (% contralateral)
40
30
20
10
0
DIO-GFP
DIO-hM4D
D
IgG extravasation (% contralateral)
100
75
50
25
0
DIO-GFP
DIO-hM4D
DIO-GFP
DIO-hM4D
E
Neurological score
5
4
3
2
1
0
*
DIO-GFP
DIO-hM4D

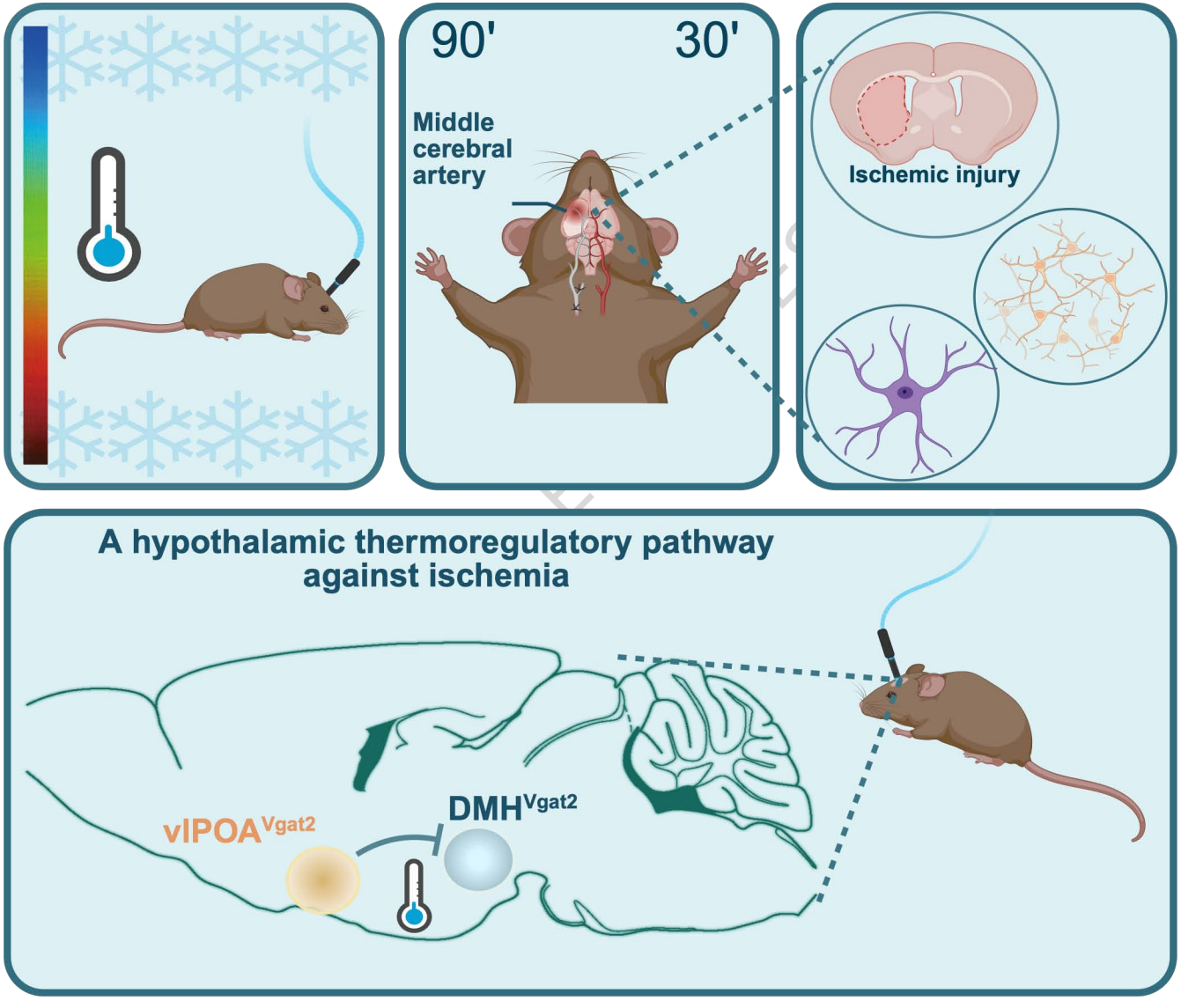

A
30 min MCAo
72 h reperfusion
Vgat-cre
B
NeuN
GFAP
Merge
DIO-GFP
DIO-hM4D
C
NeuN+ (% contralateral)
150
100
50
0
*
DIO-GFP DIO-hM4D
D
GFAP+ reactivity / hemisphere
16
12
8
4
0
*
DIO-GFP DIO-hM4D
E
PKM2
GFAP
DAPI
Merge
DIO-GFP
DIO-hM4D
F
GFAP+ / PKM2+ Mean fluorescence intensity
60
40
20
0
***
DIO-GFP DIO-hM4D
G
GFAP- / PKM2+ Mean fluorescence intensity
60
40
20
0
***
DIO-GFP DIO-hM4D


A
Baseline
MCAo
Reperfusion
0
15
45
105
Time (min)
Rostral end
Ipsilateral
Core
Penumbra
Non-injured
Contralateral
Caudal end
B
Reperfusion
Baseline
MCAo
30 min
60 min
DIO-GFP
DIO-hM4D
0
Perfusion unit
400
C
Core blood flow (% ctrl)
100
75
50
DIO-GFP
DIO-hM4D
*
BL
MCAo
Reperfusion
D
Penumbra blood flow (% ctrl)
100
75
50
DIO-GFP
DIO-hM4D
*
BL
MCAo
Reperfusion
E
TUNEL + cells/sqr.
150
100
50
0
*
DIO-GFP
DIO-hM4D
F
DIO-GFP
DIO-hM4D


A
ITR
EF1α
ChR2-eYFP
WPRE
ITR
Laser, 473 nm
DMH
VLPOA
Vgat-cre
3V
3V
F.T.
c-Fos/ChR2
B
10 Hz
DIO-GFP
DIO-ChR2
c-Fos+/eYFP (%)
150
100
50
0
**
DIO-GFP
DIO-ChR2
C
10 Hz
Tcore (°C)
38
37
36
35
34
DIO-GFP
DIO-ChR2
BL
STIM
b.s. t=60 min
ΔTcore (°C)
0
-1
-2
-3
-4
***
DIO-GFP
DIO-ChR2
D
10 Hz
20°C
37°C
DIO-GFP
DIO-ChR2


A
Infarct volume (mm3)
60
40
20
0
**
DIO-GFP
DIO-ChR2
DIO-GFP
DIO-ChR2
B
Brain swelling (% contralateral)
20
15
10
5
0
*
DIO-GFP
DIO-ChR2
C
IgG extravasation (% contralateral)
100
75
50
25
0
DIO-GFP
DIO-ChR2
DIO-GFP
DIO-ChR2
D
TUNEL + cells/sqr.
60
40
20
0
*
DIO-GFP
DIO-ChR2
E
DIO-GFP
DIO-ChR2


A
NeuN
GFAP
Merge
DIO-GFP
DIO-ChR2
B
NeuN+ (% contralateral)
100
75
50
25
0
**
DIO-GFP
DIO-ChR2
C
GFAP+ reactivity / hemisphere
6
4
2
0
**
DIO-GFP
DIO-ChR2
D
PKM2
GFAP
DAPI
Merge
DIO-GFP
DIO-ChR2
E
GFAP+ / PKM2+ Mean fluorescence intensity
60
40
20
0
***
DIO-GFP
DIO-ChR2
F
GFAP- / PKM2+ Mean fluorescence intensity
60
40
20
0
***
DIO-GFP
DIO-ChR2


90'
30'
Middle cerebral artery
Ischemic injury
A hypothalamic thermoregulatory pathway against ischemia
vlPOA Vgat2
DMH Vgat2